SHALLOW WATER EXPERIMENT UTILIZING THE STD MODEL 9006 AT A FIXED POINT

William Joseph Frigge

NAVAL POSTGRADUATE SCHOOL
Monterey, California

THESIS

SHALLOW WATER EXPERIMENT UTILIZING
THE STD MODEL 9006 AT A FIXED POINT

by

William Joseph Frigge

Thesis Advisor: Noel Boston

March 1973

Shallow Water Experiment Utilizing the STD MODEL 9006 at a Fixed Point

by

William Joseph Frigge
Lieutenant, United States Navy
B.S., United States Naval Academy, 1965

Submitted in partial fulfillment of the
requirements for the degree of

MASTER OF SCIENCE IN OCEANOGRAPHY

from the
NAVAL POSTGRADUATE SCHOOL
March 1973

ABSTRACT

An examination of the salinity sensing capabilities of the STD Model 9006 was made in laboratory and in shallow water field conditions both in Monterey Bay and at the N.U.C. Tower off Mission Beach at San Diego, California. Laboratory studies showed it to be influenced by changes in water velocity from zero to non-zero. Field studies showed that the instrument was unsuitable for sensing instantaneous microstructure fluctuations of salinity in shallow water while being held at a single depth in a wave influenced regime. Averaged over a period of ten seonds or more, however, the output of the instrument was judged to be accurate to at least the first decimal place.

TABLE OF CONTENTS

LIST OF TABLES

LIST OF FIGURES

ACKNOWLEDGEMENT

The author would like to thank Dr. Noel E. Boston and Dr. Edward B. Thornton for guidance, assistance and patience in this project.

The author would also like to express his appreciation to Mr. Dana Maberry and STG1 R. H. Desgrange, USN for their many efforts toward the successful completion of the project.

In addition, the author would also like to thank Dr. Peter M. Barakos of N.U. C. for timely information concerning internal waves in the San Diego area.

Finally, without the cooperation of LCDR J. Gossner, U.S.N. and Lt. M.A.N. Whittemore, U.S.N., my classmates and co-workers, this work could not have been accomplished.

I. INTRODUCTION

Traditionally, the oceanic parameters of salinity and temperature have been used to compute sound velocity. Variations in these parameters cause variations in sound velocity. The variance of sound velocity is related to the variance of the inhomogeneous salinity and temperature fields. This sound variance can be further related to refractive index variations, Sound therefore depends statistically on salinity and temperature statistics. The use of the inverse procedure, ie., the use of sound statistics as a measure of salinity and temperature variances would seem therefore to be a valid operation. This procedure would not yield detailed information such as specific salinities and temperatures, to be sure, but would be indicative of the statistical behavior of salinity and temperature.

A good procedure to resolve this question then would be to isolate a 2 meter cube of water and measure all parameters "in situ" and subject these data to statistical analysis. A first attempt to do this was made by Seymour (1972), Duchock (1972), and Bordy (1972), in October, 1971. Further analysis of this data were done by Haley (1972), in December, 1972. There was some question that the STD Model 9006 was not a suitable instrument for microstructure measurements of salinity. This thesis describes part of a second experiment carried out in June, 1972. The specific study examines the STD in detail

with an eye as to its suitability for reliably sensing microstructure salinity fluctuations in a near-surface environment.

II. PRE-TRIAL EXPERIMENTS

Prior to use in the field, the STD was tested to determine the degree to which its output was affected by 1.) water particle motion and, 2.) non-compensated temperature changes generated by the STD (ie, the electro-magnetic energy in the salinity sensor induction coil). The possibility of these errors existed because the manner in which the STD was designed to be used was not the method used for this experiment. Further, the position of the sensor for the temperature compensation circuit which is responsible for converting measured inductance to salinity was separated by 15 cm. from the induction coil (see Appendix A).

The STD is normally used by lowering the instrument through the water column to a specified depth and recording the continuous output. It was our plan to use the STD at a constant depth, ie, the only motion present would be that due to water motion. The presence of this motion would depend on the depth at which the instrument was placed and the amount of wave activity. It was therefore imperative to determine how this presence or absence of water particle motion affected the output. A total absence of water particle motion introduced the possibility of the second type of error. With no water particle motion, the water being measured in the induction coil could be heated by the electro-magnetic energy in the induction coil. This heating would not have been corrected by the

temperature compensation circuit of the STD because the position of the compensation circuit thermistor probe was 15 cm. above the induction coil. The magnitude of this self-heating error, if it existed, was a necessary factor to be determined prior to using the STD in the actual field experiment.

A series of three experiments, one shipboard, one pier-side and one in the laboratory was performed in order to determine the effect of water particle motion and self-heating.

A. SHIPBOARD

The first experiment was performed aboard the Naval Post-graduate School's Research Vessel, ACANIA, while moored to buoys in Monterey Harbor. The water depth was approximately 40 feet, the wind was Northwest at 6-10 knots and there was no sea running (ACANIA'S moorings are protected by the Harbor Breakwater). There was a 0-1 foot swell and additional water motion was induced by passing small craft. The STD was lowered to differing depths and held motionless while the output was visually monitored on a frequency counter. The STD output varied from 5980-6030 Hz (33.349^{o}/00-33.51^{o}/00, (Fig. 1). However since the ship was continuously rolling due to the swell present, it was impossible to determine whether these variations were due to actual salinity changes or whether they were due to the fact that as the ship rolled, it caused the STD to move up and down in the water column. The range of motion was 0.5-1.0 feet. Since the STD could not be held motionless, the effect of self-heating could not be determined.

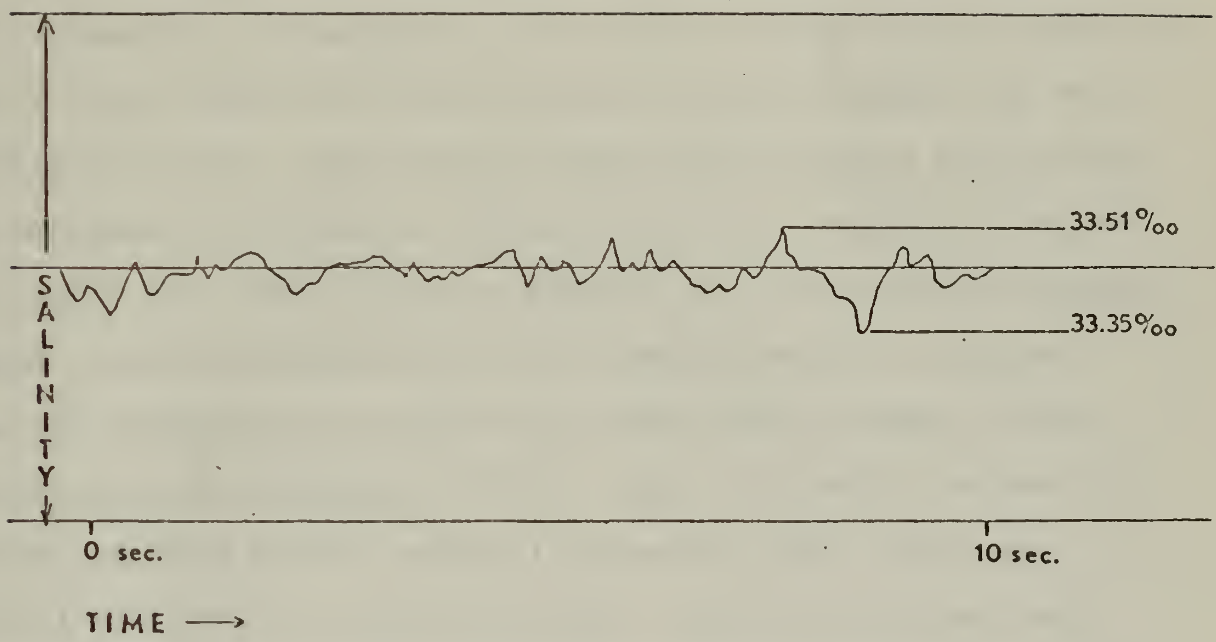

Figure 1. Results of Acania experiment.

B. PIERSIDE

The second experiment was performed off the non-protected side of the Municipal Pier at Monterey Harbor. The water depth was approximately 25 feet, the wind was west at 8-10 knots. Since the wind was offshore there was no sea. There was a 0.5-1.0 foot swell from the north and there were no small craft in the vicinity for the duration of the experiment. The STD was successively lowered to 3 feet and 20+ feet and held motionless at each depth until sufficient time had elapsed for self-heating to occur. The STD was then rapidly raised and lowered approximately one foot on either side of its original position. The output was continuously monitored by a strip chart recorder. During the motionless periods the output remained constant. When the instrument was moved the strip chart showed a fluctuation of approximately 0.2^{o}/00. When the motion ceased the output returned to its original value (Fig. 2). The same results occurred at each test depth. Since the output only varied while the STD was in motion and returned to its original value after the cessation of motion it would seem that self-heating was not a problem. If self-heating were a problem, the output should gradually increase during the motionless periods as the self-heating occurred. However, whether or not the signal fluctuation was due to actual salinity changes or to water particle motion remained unanswered.

C. LABORATORY

The third experiment was performed in the Oceanography Electronics Laboratory at the Naval Postgraduate School. A

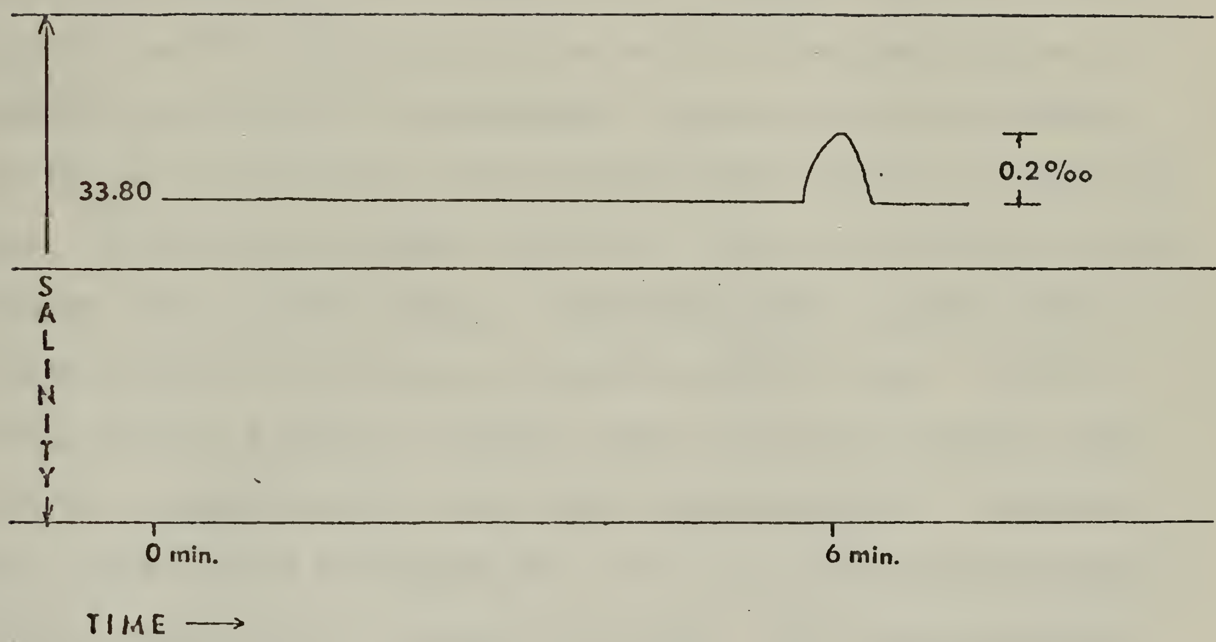

Figure 2. Results of Pierside and Lab. experiment

30 gallon container was filled with Monterey Bay Water (approximate salinity of 33.5^{o}/00 and the STD salinity sensor immersed. The salinity of the water was varied to a specific point either by diluting with distilled water or by adding a brine solution that had been made from sea salt. The test points were chosen at approximately 2^{o}/00 across the STD measurement scale, ie, 30^{o}/00-40^{o}/00. Once a test point was reached, an STD reading was obtained and then verified by a standard salinometer measurement. After this verification, the STD was checked for self-heating (same method as pierside run). This procedure was done twice. The first run was made without stirring the water. The second time a small motor-driven stirring mechanism was continually in use. In both cases, with and without mixing, and at each test point, the effects of self-heating were again non-detectable. However, when the stirring mechanism was not in use, the output signal changed values as the sensor was moved. This could possibly be attributed to salinity layering in the unmixed water. In the case of the continuously mixed water, the signal fluctuated when the sensor was moved but shortly returned to its original valve. This, as in the pierside Run, would seem to indicate that water motion through the Salinity Sensor does cause fluctuation of the output signal since the water was reasonably well mixed and therefore had a constant salinity level. The fluctuations were again on the order of 0.2^{o}/00 (approximately 50 Hz). (Fig. 2).

III. FIELD EXPERIMENT

A. LOCATION

The experiment was conducted at N.U.C. Oceanographic Research Tower. This tower, which is located approximately one mile off Mission Beach, California, was chosen for a number of reasons. It is rigidly fixed in a shallow water environment which is exposed to oceanic conditions. It is well equipped with instrumentation for physical oceanographic and other marine studies. It is convenient to marinas which allows easy access to and from the tower. Further, radio communication is maintained with N.U.C. which allows instrumentation problems to be discussed and overcome without leaving the fieldsite.

The tower is positioned in 60 feet of water (18 m.) and fixed by supporting pins driven 63 feet into the ocean floor. Electrical power is supplied by cable from a shore facility, thus insuring stable voltage and frequency. The general vicinity of the tower is free from water-borne traffic for the majority of the time. The tower itself is divided into four levels. The surface level is the entry deck and diving platform. The second level contains the winches and lifting equipment. The third level is the main work area. It has a walkway on all four sides, an equipment room and a general purpose room. The fourth level contains antennae, wind recording and solar measurement equipment. The legs of the tower

slope out five degrees. A pair of tracks is mounted on the north, south and west sides for lowering instrument packages beneath the sea surface to any depth above the ocean floor. The western side of the tower was used because of its exposure to the predominent swell.

B. INSTRUMENTATION & EQUIPMENT

The following equipment was mounted on a frame enclosing a two meter cube of water (Fig. 3).

1. Bisset-Berman STD Model 9006

a. Salinity Sensor

Time Constant	0.35 msec
Output	0.10 mv DC
Salinity Range	33-35 ppt (channel 3)
Accuracy	± .02 ppt

b. Temperature Sensor

Time Constant	0.35 sec
Output	0-10 mv DC
Temperature Range	14^{o}-19^{o} C
Accuracy	± 0.02 ^{o}C

c. A detailed description of this instrument is presented in Appendix A

2. Thermistors (6)

Time constant	150 msec
Output	305 mv/^{o}C
Temperature Range	10^{o}-21^{o} C

A detailed description of the thermistor system is given by Whittemore (1973).

3. Ramsay Corporation Mark I SVTD

Time Constant	160 microseconds
Output	0-10V DC
Accuracy	± 0.01 m/sec

A detailed description of this instrument is given by Gossner (1973).

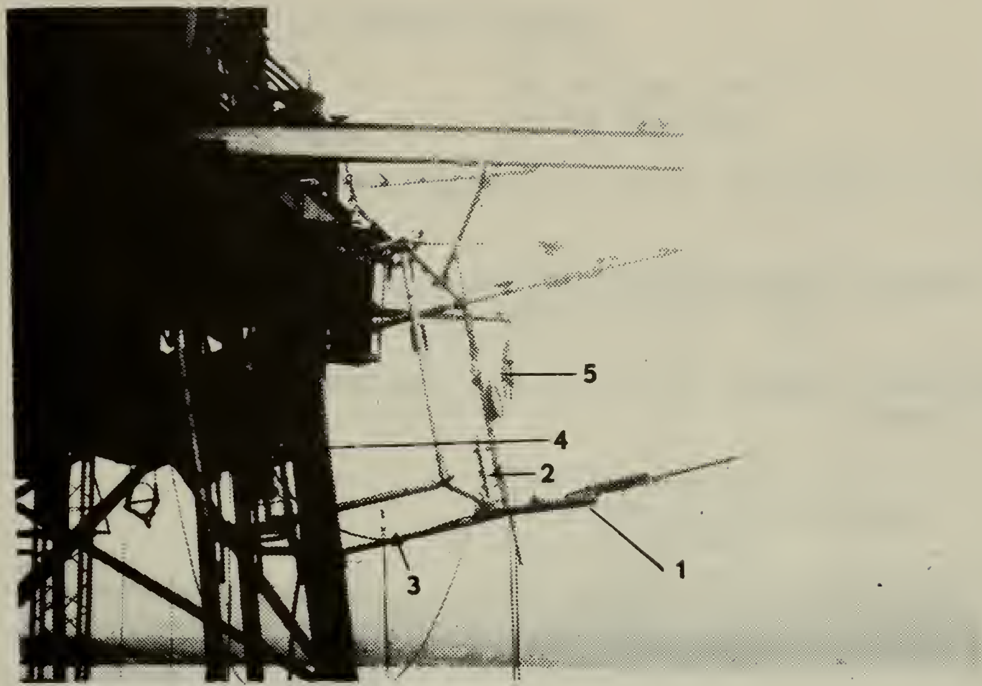

INSTRUMENT RACK AND TOWER

INSTRUMENTS

1.) FLOW METER

2.) RAMSAY PROBE

3.) THERMISTOR

4.) STD

5.) WAVE GUAGE

Figure 3. Instrument Rack and Placement

4. Baylor Wave Height Sensor

Output	50 mv/foot of ht.
Accuracy	1% of reading

A detailed description of this instrument is given by Krapohl (1972).

5. Particle Velocity Sensor (Engineering Physics Company Water Current Meter Model EMCM - 3B)

Time constant	0.2 sec or longer (adjustable by user)
Accuracy	The largest of 1) ± 1% of full scale 2) ± 5 mm/sec 3) 5/(T½) mm/sec (T=Time Constant)

This instrument also is described in detail by Krapohl (1972).

Data were recorded on a Sangamo Magnetic Tape Recorder Model 3562. Of its 14 channels, 11 channels were allocated for recording oceanographic parameters.

The channel allocations were

(1) Flowmeter
(2) Flowmeter
(3) Waveheight
(4) Not used
(5) Not used
(6) Ramsay sound velocity
(7) Ramsay temperature
(8) B-B STD salinity
(9) B-B STD temperature
(10) Synchronization
(11) Thermistor
(12) Thermistor
(13) Thermistor
(14) Voice

C. ENVIRONMENTAL CONDITIONS

A resume of environmental conditions, by run, is given in Table I.

TABLE I

METEOROLOGICAL DATA								BT DATA	
Run #	Time Local	Cloud Cover (%)	Wind Direc.	Wind SPD (kts.)	Swell Direc.	Air Temp. (°F)	SFC Temp. (°F)	1st Layer Temp. (°F) Depth (ft.)	2nd Layer Temp. (°F) Depth (ft.)
1	1405	100	WSW	8	W	67.5	66.5	72/24	62/40
2	1600	100	WSW	10	WSW	67.3	66.0	72.10	68/42 63/52
3	1654	100	WSW	9	WSW	66.5	64.8	74/20	71/30 69/54
4	1800	100	WSW	6	SW	65.6	66.4	70/16	67/22 65/58
5	1830	100	WSW	7	SW	64.2	66.0	71/18	68/36 66/56
6	1922	100	WSW	4	SW	64.0	65.7	68/19	
7	2000	100	WSW	4	SW	63.8	65.4	BT Malfunctioned	
*8	0837	100	WSW	4	SW	63.1	65.7	61/28	
*9	0935	100	WSW	8	SW	63.5	65.3	61.31	
*10	1000	100	WSW	4	SW	65.8	65.3	61/30	

Runs 1-7 Conducted 8 June 72
*Runs 8-10 Conducted 9 June 72

The presence of internal waves in the general area was recognized. Information concerning this phenomenen is well documented (Barakos, 1972). In addition, a high tide of 5 ft. occurred at 1928 local time (in run #6) and again at 0801 (shortly before run #8).

D. EXPERIMENTAL CONFIGURATION

The STD was mounted vertically on the tower end of the cubic frame (Fig. 3), parallel to the tower track with the salinity sensor in the bottom horizontal plane of the frame. The Ramsay Probe was amounted with its sensors in the same plane, however, it was at the front left (looking seaward from the tower) seaward end of the frame. The thermistor probes were mounted in the same bottom horizontal plane, but in a line along the left side of the frame. The water current meter was mounted at the seaward end, center, of the frame in the bottom horizontal plane. The Baylor wave guage was mounted vertically from the top horizontal plane of the frame to the bottom horizontal plane. It should be noticed that all instrumentation, with the exception of the wave guage, was located in the bottom horizontal plane of the frame. Thus, any measurable characteristic of the water in that plane should have been recorded by all the instruments.

In addition, hydrophones and receivers were mounted on the frame by acousticians who were conducting experiments related to sound amplitude modulation, sound dispersion and phase fluctuations (Fitzgerald, 1972 & Alexander, 1972).

E. GEOMETRICAL & INTERFERENCE CONSIDERATIONS

The various sensors were mounted as described in Section D and shown in Fig. 3, in order to reduce the effects of mutual interference between sensors, especially those in the sound propagation path between hydrophone and receivers.

F. EXPERIMENTAL PROCEDURE

Whenever possible equipment was checked out in the laboratory before transportation to San Diego. Upon arrival in San Diego the equipment was taken to the tower, assembled on deck and tested to insure no damage occurred during shipment and handling. The equipment was then mounted on the frame at locations chosen on the basis of spatial resolution of the parameters measured. This of necessity involved some compromising of the ideal theoretical locations. After the equipment was mounted on the frame, it was lowered to a preselected depth. The equipment was then energized and signals examined via strip chart and oscilloscope monitoring. When signal levels were appropriate for the tape recorder input, the data were recorded for the desired length of time. The signals on each of the recorder channels were periodically monitored to insure as far as possible that none of the equipment was malfunctioning and that signals did not exceed the dynamic range of the tape recorder. In addition, while the data were being recorded, weather observations were being recorded, BT casts made and water samples taken. Care was exercised to insure that these water samples were taken from

the depth at which the sensors were located for that particular run. The samples were used to verify the output of the salinity and temperature sensors. At the conclusion of the run the equipment was de-energized, the frame repositioned and the procedure repeated for the next run. The length of the average run was approximately 20 minutes. The choice of depth to which the frame was lowered for a specific run was generally governed by the depth of the thermocline and the need to gather "<u>in situ</u>" data from regions of maximum and minimum water motion, ie, deep and shallow depths.

IV. DATA COMPILATION AND RUN DESCRIPTION

A. TABLE OF MEASURMENTS

Run	SST	Salinity	Sound Velocity
1	18.24	33.85	1515.24
2	16.87	33.74	1511.63
3	16.97	33.75	1511.68
4	16.70	33.76	1511.17
5	17.71	33.89	1513.79
6	17.12	33.83	1510.57
7	17.32	33.84	1511.62
8	17.34	33.89	1513.63
9	12.72	33.83	1498.52
10	12.87	33.97	1409.32

TABLE II.

B. RUN DESCRIPTION

Run #	Time Start	Depth Instruments/Thermocline	Tape Length Start/Finish
1	1405	18.7/24	62/296
2	1600	41.3/10	310/522
3	1654	34.8/20	535/1045
4	1800	28.4/16	1061/1294
5	1830	21.8/18	1322/1499
6	1922	14.3/19	1520/1703
7	2000	14.3/*	1719/1845
8	0837	14.3/28	1879/2165
9	0935	47.3/31	2181/2370
10	1000	29.8/30	2398/2743

*BT Malfunctioned

TABLE III.

V. DATA REDUCTION

A. PROCEDURE

Data from the instruments were recorded on the Sangamo Model 3562 fourteen channel tape recorder for the ten data collection runs. The analog FM recordings were then transcribed onto a rectilinear eight channel strip chart recorder after amplification through operational amplifiers on a Ci Model 5000 analog computer.

B. STRIP CHART ANALYSIS

1. The data for each of the ten runs were displayed on the strip chart for purposes of qualitative examination and editing.

2. The strip chart analysis showed that several records were not suitable for either digitization or for qualitative analyzation for a number of reasons. Among them are: clipped signals, short data sections interrupted by gain changes and/or equipment malfunction. At other times problems resulted from a sudden change in environmental conditions, usually internal waves, thus destroying the stationarity of the parameters. The runs not analyzed because of such problems were runs #2, #3, #4, #8 and #10.

3. Some records showed interesting but short lived signals which were usually well correlated with each other. However, because of their transient nature they were not suitable for digitizing. Rather, more direct calculations were made in an

attempt to describe their occurence. Such cases were found in runs #1 and #9.

4. Those signals which showed reasonably strong signals throughout the run were digitized and then analyzed on the IBM 360/67.

C. ANALOG TO DIGITAL CONVERSION

1. Procedure

Those runs selected for analysis were digitized using a hybrid system that consisted of the Ci 5000 Analog Computer and a Zerox Data Systems Model 9300 Digital Computer. After digitizing onto the seven track tape used by the 9300 the data were transcribed onto a nine track tape using the Postgraduate Schools' IBM Model 360/67 Digital Computer. The tape and computer were subsequently used for the statistical analysis of runs #5, #6 and #7.

2. Conversion and Statistical Analysis Parameters

Each run analyzed had six signals of interest: temperature, T1, from a thermistor, sound velocity from the Ramsay probe, salinity from the STD, a u component and a v or w component of the particle motion from the flowmeter and sea surface height from the wave guage. The digital sampling rate for each of these analog signals was five samples per second. This defined the high frequency limit (Ref. 11).

$$\Delta t = 1/\text{sample rate} = .2 \text{ sec.}$$

$$f_h = 1/2\Delta t = 2.5 \ H_z$$

This frequency is commonly known as the "cut-off frequency", "Nyquist frequency". Each data run was divided into a number of

records by the 9300. The number of records depended on the time length of the run. Each record contained 512 data pieces. Of the runs to be analyzed, run #5 had twelve records (512 x 12 = 6144 data pieces), run #6 had the same and run #7 had 7 records (3584 data pieces). The lowest frequency that can accurately be distinguished is a function of the length of record, T, of the data being analyzed (Ref. 11). In order to have some statistical reliability in low frequency data at least ten cycles should exist in the record. Since the average record length was 20 minutes then in each record the maximum period of interest was:

20 min. per record/10 cycles per record =2 min. per cycle

This yielded a low frequency limit of

f_l = 1/T max. = 1/120 sec. = .0083, thus the frequencies to be analyzed were .0083 - 2.5 h_z (f_l - f_h). It was recognized that the lower end of this spectrum might be affected by internal waves.

VI DATA ANALYSIS

A. OBJECTIVES

The principle objective of this investigation was to determine how salinity variations compared with variations of other parameters (ie, sound velocity, temperature, water particle motion and waves). However, the results of the pretrial experiments (Sec. II) introduced the question as to whether the STD was a suitable instrument for use in measuring salinity fluctuations over the space and time scales for which the experiment was designed. Furthermore, was it suitable to use for constant depth measurements since the instrument was designed not to be fixed in space but for vertical traverses through the water column?

Determining answers to these questions is not trivial either in the laboratory or in the ocean. The laboratory experiments have been described already and strongly indicate that the STD is velocity sensitive. In order to determine the degree to which this effect would show in oceanic data a variety of statistical approaches were employed. Necessarily, assumptions are immediately imposed which may not always be valid in the complex surface region of the ocean. Specifically, the medium was considered to be homogeneous in the horizontal thus allowing stationarity to be invoked. Where this was clearly violated, statistical analyses were not performed and a qualitative approach was adopted.

B. STATISTICAL PROGRAMMING

Spectral analysis was performed on the data. The program used, along with examples of constant inputs, is in the Computer Program Section. The spectra were computed by fourier transforming caluclated covariance. The Parzan window is applied to the covariance functions to account for the finite length of records.

C. QUALITATIVE DESCRIPTION

1. Statistical Analysis

BT traces and sensor/frame location for the statistically analyzed runs are shown in Fig. 4. It should be noticed that Run 5 has the sensor at a deeper location (22 ft.) than runs 6 and 7 (both at 14 ft.). Meteorological and Oceanographic observations are included on the respective BT traces.

a. Phase Relationships.

Almost all plots indicate random phase relationships. In all cases, run 7 is less variable than runs 5 and 6. This suggests that the medium in which the instrumentation of run 7 was placed was not as homogeneous as it was in runs 5 and 6. Large scales were present without small scales. This could be interpreted as a turbulently inactive region such as the thermocline, where small scale salinity gradients have diffused. The BT slides for runs 5 and 6 (Fig. 4) show that the instrumentation was above the thermocline in both cases. Unfortunately the BT malfunctioned on run 7 so the instrumentation cannot be accurately determined relative to the thermocline. However, as can be seen from the

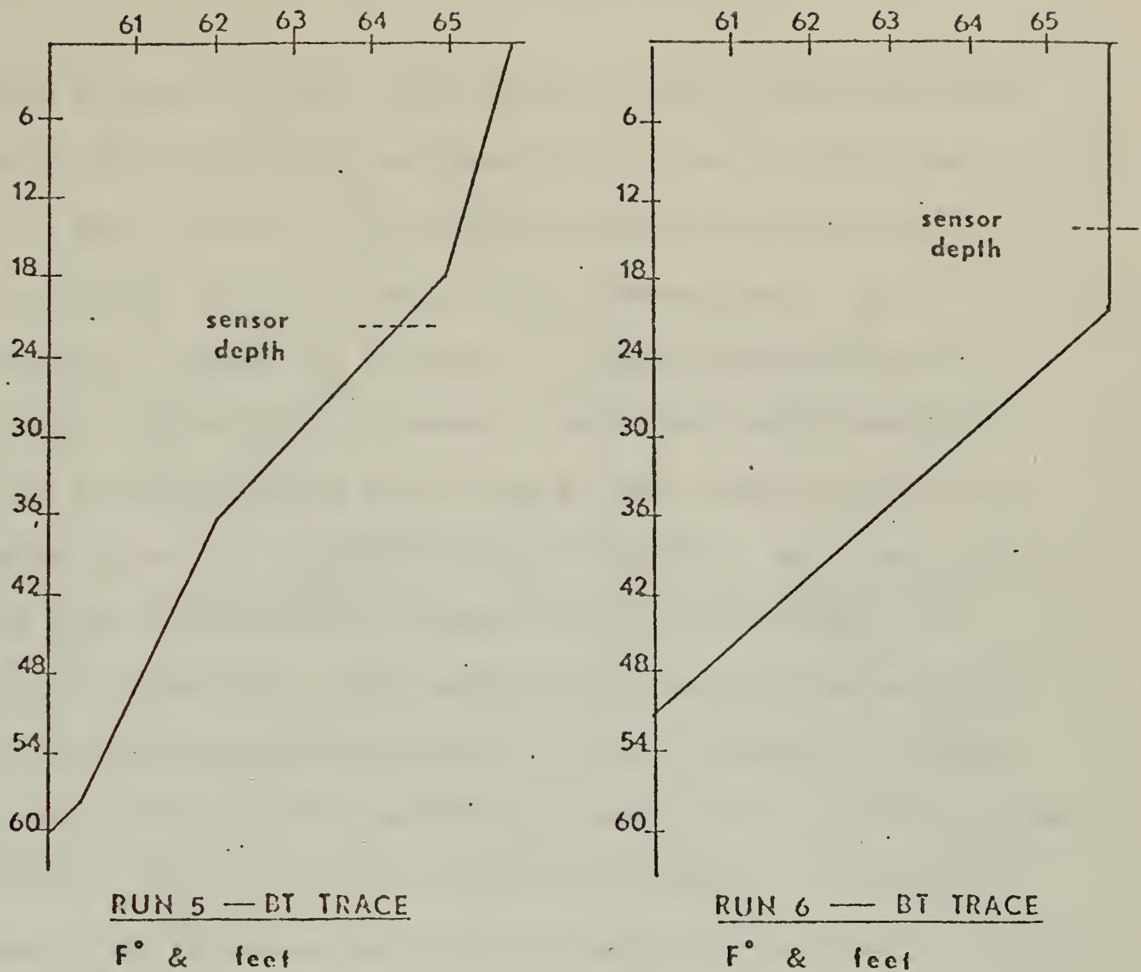

100%	Cloud cover	100%
7 kts.	Wind speed	4 kts.
WSW	Wind direction	WSW
SW	Swell direction	SW
64.2 °F.	Air temp.	64 °F.
66.0 °F.	Water temp.	65.8 °F.

Figure 4. BT traces and environmental conditions of digitized runs

BT traces of runs 5 and 6, the depth of the thermocline was decreasing and since the instrumentation was at the same depth for runs 6 and 7, it could very well be that the instrumentation in run 7 was in the thermocline. This, unfortunately, cannot be proven. If the instrumentation were in the thermocline, however, the phase relationships of run 7, as compared to run 5 and 6, are easily explained. The thermocline is a region of high stability and therefore would be less susceptible to small scale variations, ie, turbulence. Therefore, the number of fluctuations per unit time detected by instrumentation in the thermocline would be much less than that detected by instrumentation not in the thermocline. This is only a proposal, however, since the whereabouts of the instrumentation cannot be accurately placed relative to the thermocline. Appendix (B) contains phase plots for all parameters and runs.

b. Energy Spectra.

The energy spectra are, at first glance, singularly uninteresting. The peaks in runs 6 and 7 are clearly wave dominated and do not appear in run 5 which is the deepest of the three runs.

Since wave energy is evident these spectra suggest either 1.) the STD is responding to wave motions and interpreting wave motions as salinity variations or 2.) salinity is advected by waves. Of the two possibilities the former is more likely since the medium is essentially isohaline throughout and salinity values did not signi-

ficantly vary with time. In order for the second case to be true a salinity gradient of 0.1 - 0.2 ^{o}/oo would have to have been advected past the STD. Since, no such gradient existed, these spectra provide damaging evidence as to the ability of the STD to perform fixed point salinity measurement in the near surface region. Appendix (C) contains Energy Spectra for all runs and parameters.

c. Coherence Relationships

Table IV summarizes the coherence relationships. Coherence ranges from 0 to 1, the latter being perfect coherence. The frequency range over which the coherence relationships were calculated was 0-2.5 hz. The values given in the table show first the coherence and then the frequency at which that coherence was obtained (ex. Coherence/hz.).

PARAMETER	Run 5 Co/hz	Run 6 Co/hz	Run 7 Co/hz
Sal vs. SV	0.604/1.252	0.361/0.057	0.554/0.065
Sal vs. Tl	0.332/0.102	0.601/0.062	0.542/0.073
Sal vs. U-pm	0.279/2.180	0.47 /0.062	0.514/0.065
Sal vs. V&W pm	0.286/0.133 &2.170	0.562/0.062	0.610/0.065
Sal vs. SSEL*	0.328/1.430	0.550/0.062	0.489/0.065

*Sea surface elevation, ie, wave HT.

TABLE IV

It is immediately apparent that runs 6 and 7, the shallow runs, show remarkable similarity in both the amount of coherence and the frequency at which it occurred. This frequency corresponds to a period of 15-16 seconds. The calculated wave spectra show

that the average wave period corresponding to the frequency of maximum energy present during the experiment was 17.1 seconds. Run 5, the deepest of the runs, however, showed little. Appendix (D) contains coherence plots for all runs and parameters.

2. <u>Qualitative Summarization of Pre-Trial Experiments</u>

a. The shipboard experiment (sec. II, part A) showed a continual fluctuation of the STD output of approximately 0.2 ^{o}/oo (Fig. 1). However, the ship was continually in motion for the duration of the experiment and thus no information could be obtained about the STD output when it was held motionless.

b. The pierside experiment (Sec. II, part B) showed a fluctuation of STD output of approximately 0.2 ^{o}/oo only when the sensor was in motion (Fig 2). In this experiment the absolute salinity values were not monitored by any means other than the STD and the salinity remained constant when the STD was not in motion.

c. The laboratory experiment (Sec. II, part C) also showed a fluctuation of approximately 0.2 ^{o}/oo only when the sensor was in motion, (Fig. 2). This occurred both when the water was unmixed and when it was well mixed. Again the output signal remained constant when the STD was motionless.

Some velocity sensitivity is certainly to be expected for this type of instrument. It is not a unique problem and occurs for most temperature sensors. The troubling aspect is

that the fluctuation, 0.2 ^{o}/oo, is too large to be ignored or even removed analytically. The evidence is again strong that significant salinity variations are indicated when flow past the sensor changes from still to a non-zero value, ie, during the transition stage from no motion to some finite motion. This suggests that the STD be used only in motionless water or in water moving faster than some threshold value. Near the surface wave motion goes from forward to stop to reverse and repeats this continually. This is perhaps then the worst regime in which to use the STD fixed in space. The causes can be due to the compensating thermistor being velocity sensitive or a mismatch in the response times of the conductivity cell and the compensating thermistor.

The velocity sensitivity of the thermistor would depend on its overheat. The overheat difference between ambient water and thermistor bead temperature depends on the current flowing through the bead. If the current is too large, the motion of the water cools it, causing its resistance to change and hence the voltage drop across it. In effect, one has a "hot bead" thermistor, a direct analogy of the hot wire anemometer. According to the instrument specifications, the resistance of the compensation circuit is 100 ohms at 20^{o}C and the current supplied to the salinity sensor is 40 ma. With this general information one cannot readily calculate power loss, ie, overheat, in the circuit. In order to do so, one would have to disassemble the salinity

sensor and take a measurement with an A-C ammeter on the compensation circuit with the sensor energized and immersed in a bath with the temperature controlled as closely as possible to that in which the field work is to be done. One would also have to take a resistance reading of the circuit if the temperature of interest differed from the advertised 20°C. These figures could then be compared with manufacturers designed heat dissipation figures if they were, in fact, available.

The mismatch between the compensation thermistor and conductivity cell is well known, ie, the thermistor time constant being 0.35 sec. and the conductivity cell being essentially instantaneous. Briefly, the conductivity cell can respond more quickly to conductivity changes than the compensation circuit can respond to temperature changes. Since salinity is computed from conductivity and temperature and the system is analog, ie, uses a continuous information flow, the salinity computed at any given time will be erroneous if either of the inputs is erroneous. With the relatively large time constant of the thermistor, its input to the salinity signal will always be less than the actual temperature in regions of a temperature gradient and thus the salinity signal itself will be erroneous in those regions.

3. Qualitative Description of Runs 1-4 and 8-10

Run #1: Depth: 10 ft. Sensors above Thermocline

Salinity, temperature and sound velocity fluctuations are large in magnitude and over periods of 5-6 minutes correlate well with water particle motion and sea surface elevation.

Run #2: Depth: 43 ft. Sensors in Thermocline

Very significant decrease in magnitude of fluctuations of salinity, temperature and sound velocity as compared to run 1. No correlation discernable over any specific periods between any of the parameters.

Run #3: Depth: 36 ft. Sensors in Thermocline

Very significant decrease in magnitude of fluctuations of salinity, temperature and sound velocity as compared to run 1. However, all sensors do agree on the presence of some type of phenomenon, very probably an internal wave, with a period of approximately 1.8 minutes. Other than this, there was no discernable correlation between parameters.

Run #4: Depth: 28 ft. Sensors below Thermocline

Very significant decrease in magnitude of fluctuations of salinity, temperature and sound velocity as compared with run 1. No discernable correlation between parameters.

Run #8: Depth: 18 ft. Sensors in Thermocline

Salinity, temperature and sound velocity fluctuations are large in magnitude. Some degree of correlation discernable between those parameters and that of water particle motion. Some evidence of a long period phenomenon recorded by salinity, temperature and sound velocity sensors that

is not recorded by particle motion and wave height sensors. Again, very probably an internal wave.

Run #9: Depth: 40 ft. Sensors below Thermocline

Significant decrease in the magnitude of fluctuations of salinity, temperature and sound velocity as compared to run 8. No discernable correlation between parameters.

Run #10: Depth: 18 ft. Sensors in Thermocline

Unable to display this run on strip chart for analysis purposes due to problems encountered during recording of data.

D. ANALYSIS

The results of the pre-trial experiment (Sec. VI, part C, para. 2) indicated that while self-heating was not going to be a problem with the STD, there was more than a slight possibility that it was susceptible to water particle motion. The qualitative description of the non-digitized runs tended to confirm this possibility. It showed that the position of the sensors relative to the thermocline had no bearing on the magnitude of the fluctuations recorded by the STD. It also showed that when the STD was at a depth of 18 feet or less, the magnitude of the fluctuations of the salinity signal increased significantly. This depth dependence, or more accurately, water particle motion dependence of the STD was further borne out by the results of the statistical analysis (Sec.VI,part.C, para. 1, sub-para. c.). This showed a maximum coherence of .5-.6, centered at the period of the waves that were present during the experiment.

When the STD was at a depth of approximately 22 ft. the coherence was very low. With this information in hand it would seem safe to state that the STD output is affected by water particle motion. Since this is the case, it does not appear that one can hang the STD at a fixed depth in a region of water particle motion and gather accurate data on salinity fluctuations. In the case of our experiment, the depth at which the STD was not affected by water particle motion was between 18 and 23 feet. This depth would naturally vary depending upon wave characteristics at the time of measurement.

Despite the previous maligning of the instrument, it must be stated, in all fairness, that when the STD signal was averaged over a time period in any given run, the results coincided to at least the first decimal with those salinity values obtained by the bench salinometer. In addition, Gossner (1973) used a ten minute averaging period of STD salinities in his work of comparing measured and computed sound velocity. The results showed that STD measured salinity values could be utilized in Wilson's Equation in obtaining sound velocity values that were accurate to 0.1 m/sec.

VII. CONCLUSIONS

1. The STD Model 9006 is unsuitable for in-place microstructure measurements.

2. The STD Model 9006 is unsuitable for microstructure measurements where a variable velocity water particle motion exists.

3. STD Model 9006 output is unreliable in a region of high salinity and/or temperature gradients.

4. Macrostructure values of STD Model 9006 output when averaged over a 10 minute time period, are accurate to at least the first decimal place.

APPENDIX A

GENERAL DESCRIPTION OF PLESSY ENVIRONMENTAL SYSTEMS - MODEL 9006 SALINITY, TEMPERATURE AND DEPTH MEASURING SYSTEM

The model 9006 STD is comprised of underwater sensors and deck equipment. The function of the deck equipment is to furnish power to the sensors and process data received from same.

"*In situ*" measurement of salinity is determined by measuring conductivity, temperature and pressure. An inductively-coupled sensor enables detection of conductivity, which is also compensated for temperature and pressure effects, thereby producing an output totally dependent upon salinity. The output shifts the frequency of a PARALOC signal providing an FM analog of salinity

The temperature sensor uses a platinum resistance thermometer and a PARALOC which provides an FM analog of temperature.

The depth sensor utilized a pressure transducer into which is incorporated into a strain-gauge bridge circuit. The changes in resistance are converted to a frequency analog in the PARALOC.

The signal mixer receives and regulates power from the deck equipment and sends it onto the underwater sensors. It then multiplexes and amplifies the FM signals from the sensor and sends them to the deck equipment.

The distribution amplifier amplifies the FM signal from the underwater units, and separates data signals from the DC power. The signal then enters the distribution amplifier from the power supply rack.

Each underwater sensor has a separate discriminator which separates the mixed data signal into an individual channel for recording availability. The discriminator filters the desired signal and rejects others. The accepted signal is amplified, squared, and converted to a 0-10 millivolt DC level which is the output of the recorder. Dial readouts enable continual monitoring of this signal.

The Power Supply is a model 8600 and provides a constant voltage of 26.5 volt DC to the deck units, and a constant current of 150 milliamps at a maximum of 140 volts DC to the underwater units. The underwater rack is stainless steel. The sensors and mixer are mounted in individual shock-absorbent brackets.

A single conductor cable provides for physical connection between sensors and deck equipment.

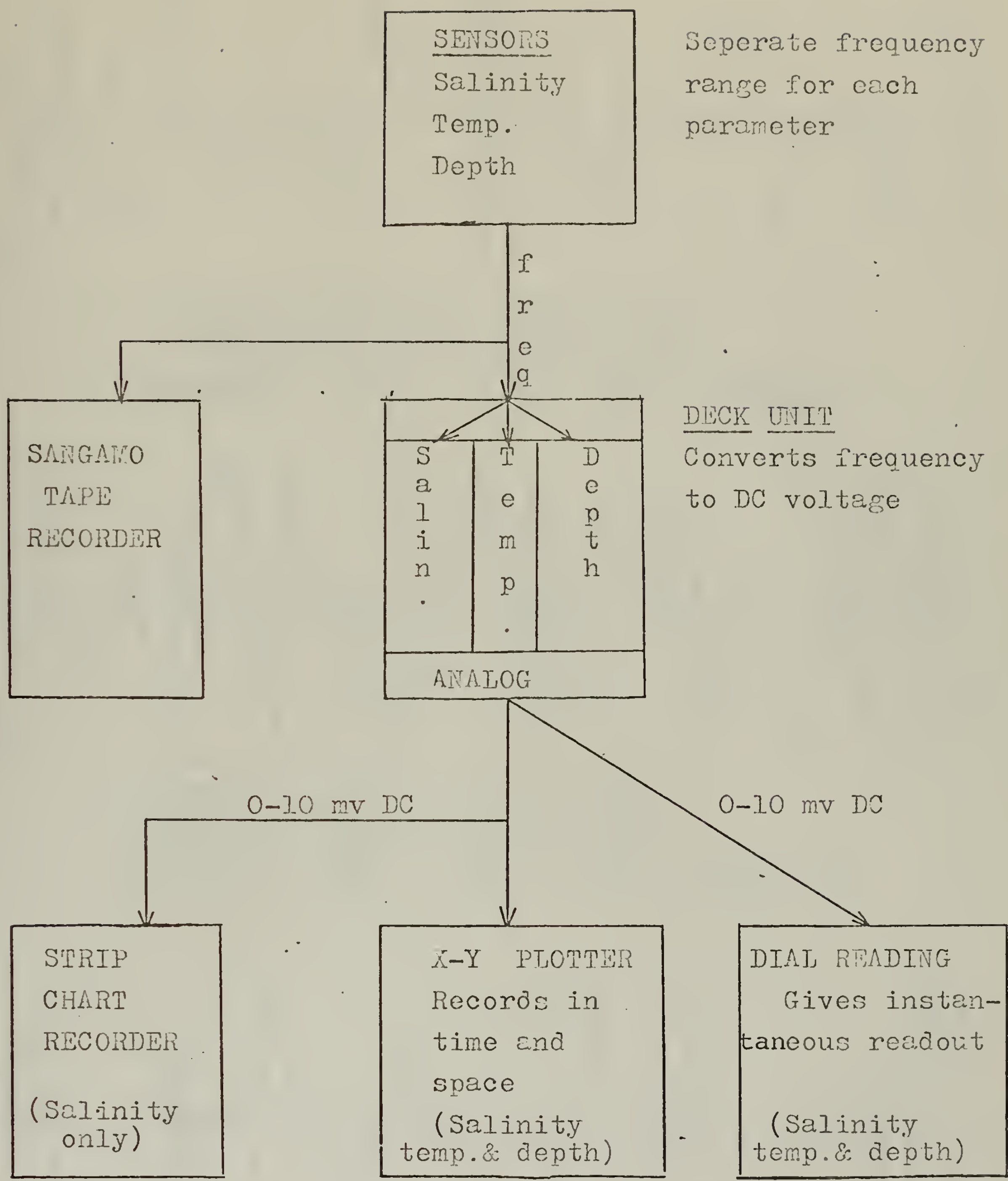

FIGURE 5 Flow Diagram of STD Model 9006

PHASE RELATIONSHIPS

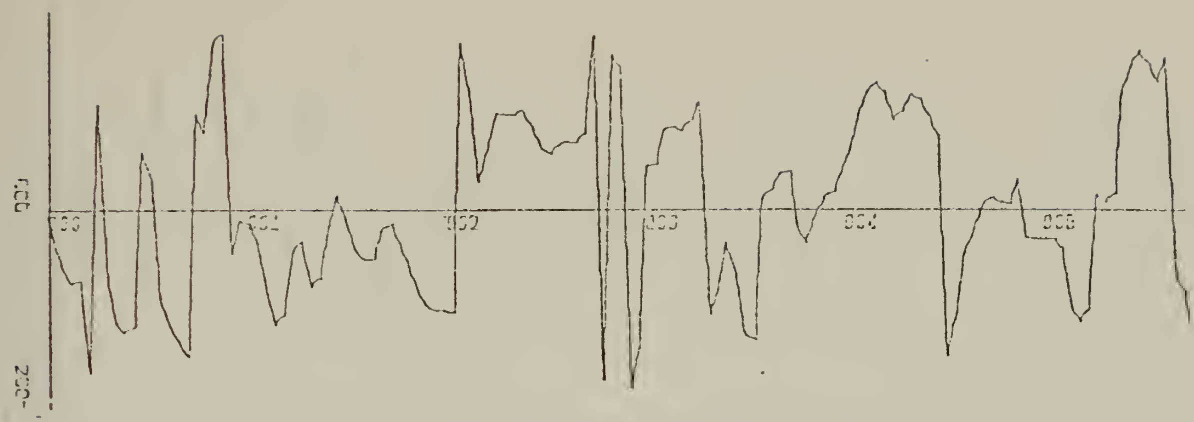

X-SCALE=1.00E-01 UNITS INCH.
Y-SCALE=2.00E+02 UNITS INCH.
PHASE-SAL. VS. SV. RUN 5

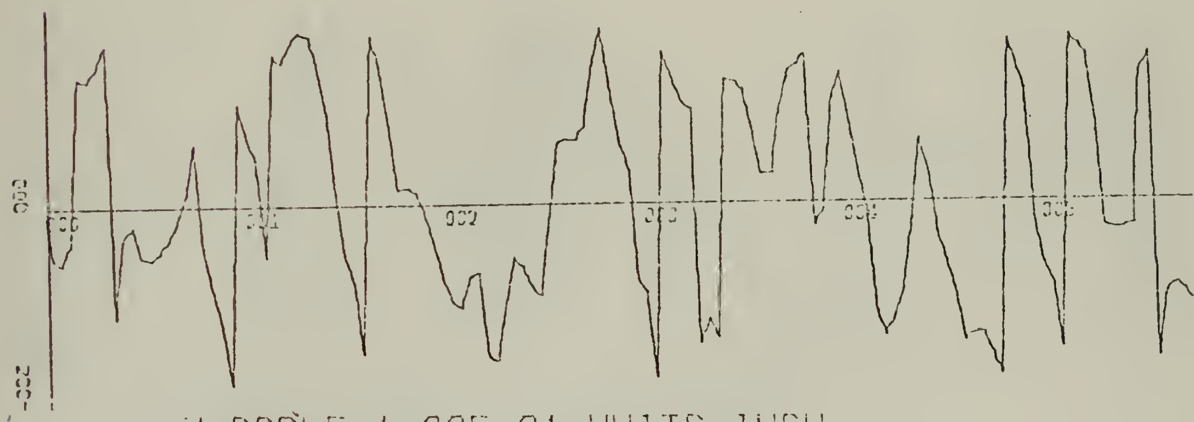

X-SCALE=1.00E-01 UNITS INCH.
Y-SCALE=2.00E+02 UNITS INCH.
PHASE-SAL. VS. SV. RUN 6

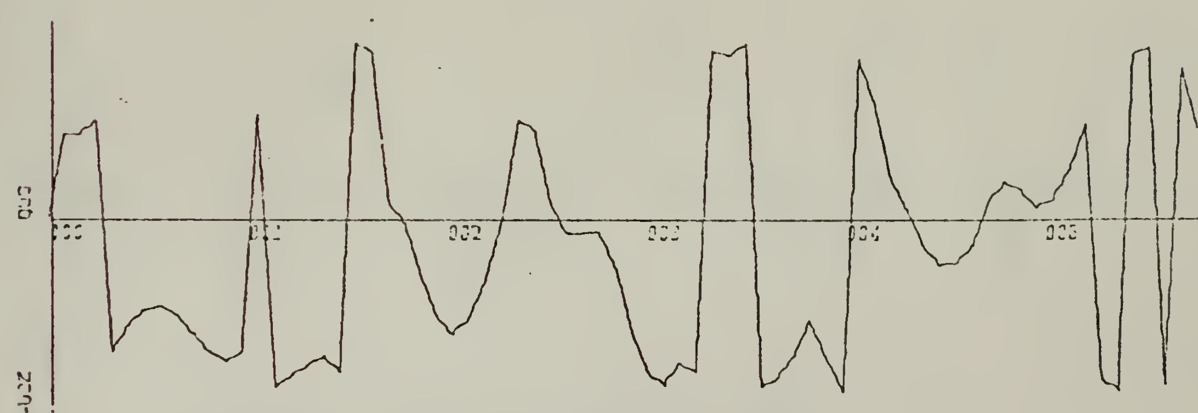

X-SCALE=1.00E-01 UNITS INCH.
Y-SCALE=2.00E+02 UNITS INCH.
PHASE-SAL. VS. SV. RUN 7

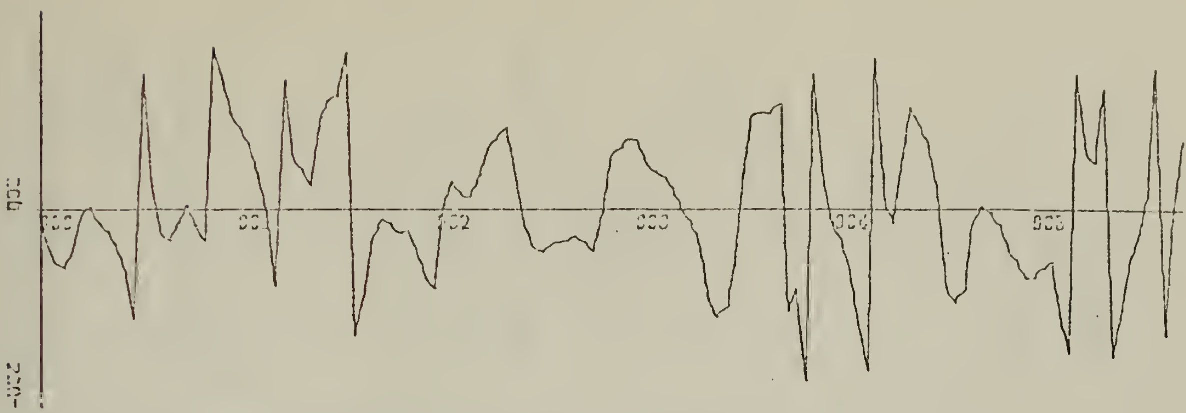

X-SCALE=1.00E-01 UNITS INCH.
Y-SCALE=2.00E+02 UNITS INCH.
PHASE SAL. VS. T1RUN 5

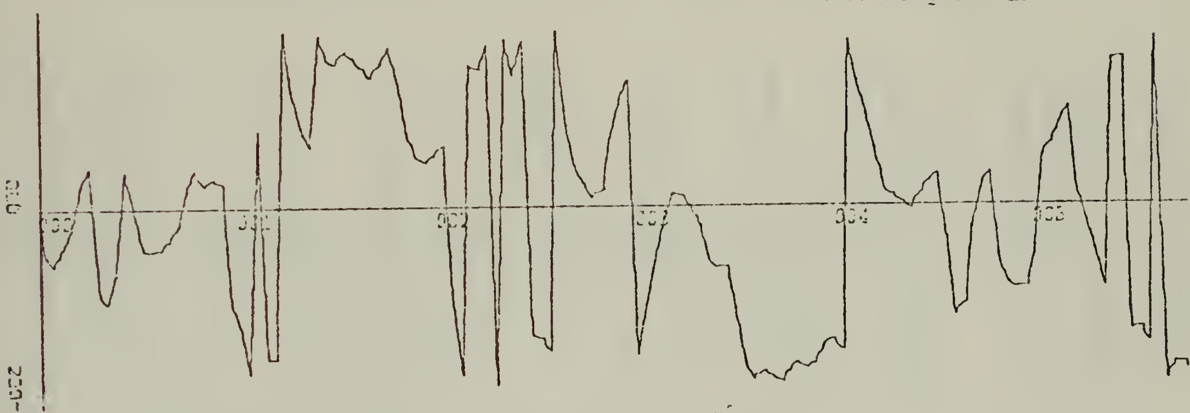

X-SCALE=1.00E-01 UNITS INCH.
Y-SCALE=2.00E+02 UNITS INCH.
PHASE SAL. VS. T1 RUN 6

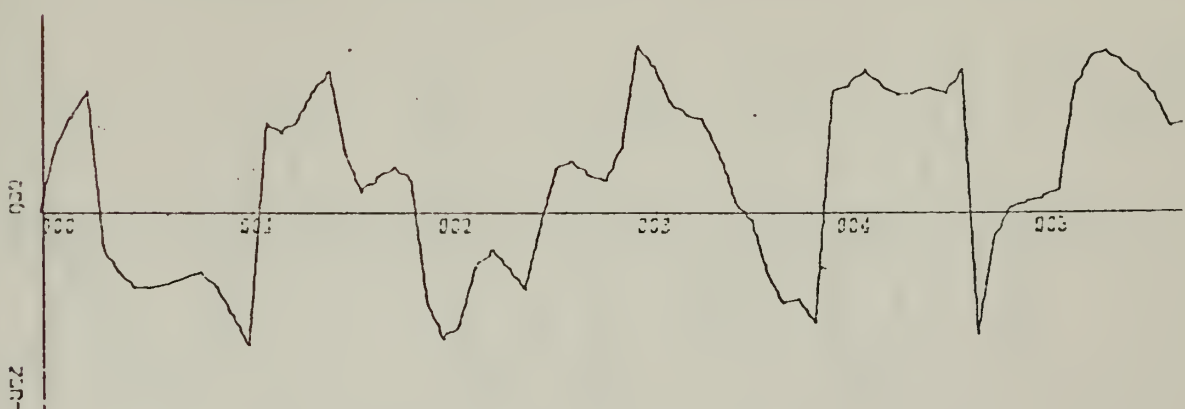

X-SCALE=1.00E-01 UNITS INCH.
Y-SCALE=2.00E+02 UNITS INCH.
PHASE SAL. VS. T1 RUN 7

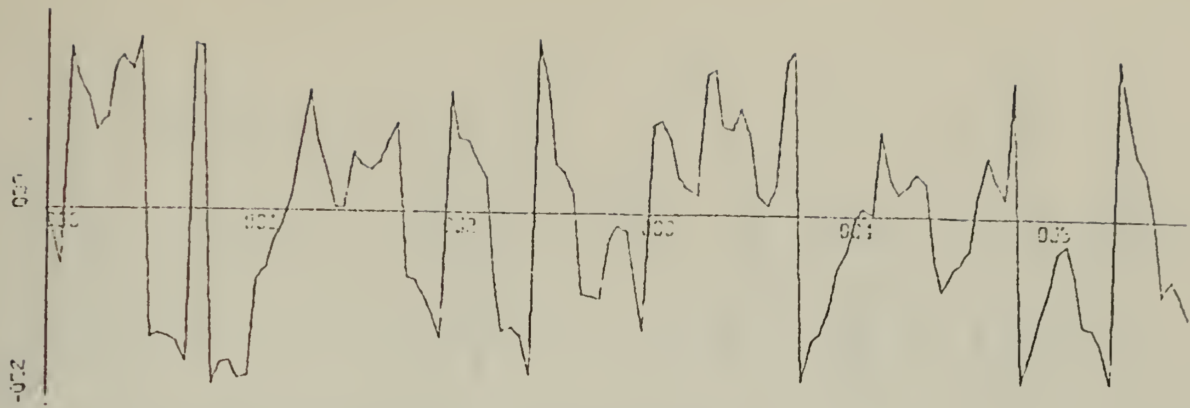

X-SCALE=1.00E-01 UNITS INCH.
Y-SCALE=2.00E+02 UNITS INCH.
PHASE SAL. VS. U-PM RUN 5

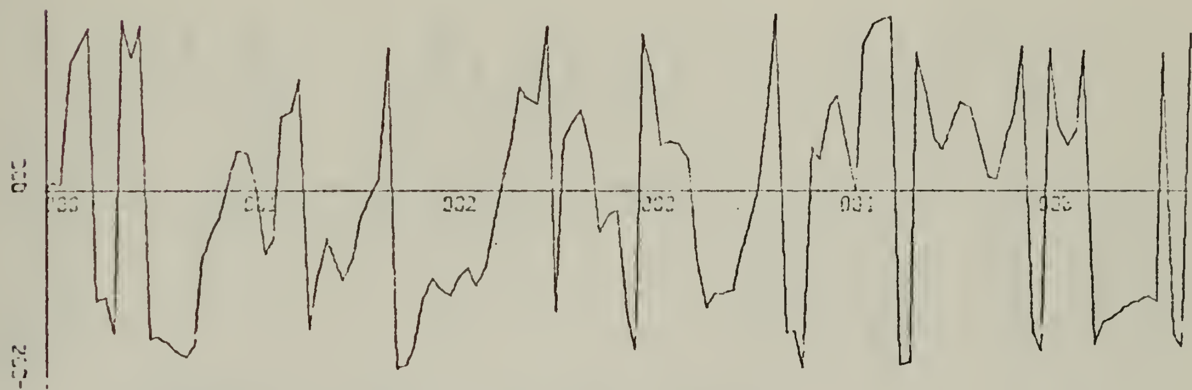

X-SCALE=1.00E-01 UNITS INCH.
Y-SCALE=2.00E+02 UNITS INCH.
PHASE SAL. VS. U-PM RUN 6

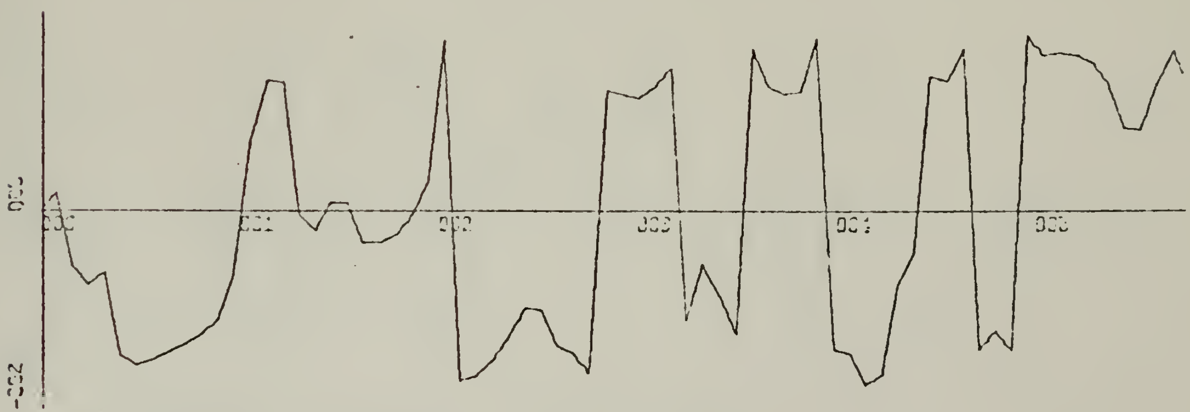

X-SCALE=1.00E-01 UNITS INCH.
Y-SCALE=2.00E+02 UNITS INCH.
PHASE SAL. VS. U-PM RUN 7

X-SCALE=1.00E-01 UNITS INCH.
Y-SCALE=2.00E+02 UNITS INCH.
PHASE SAL. VS. W-PM RUN 5

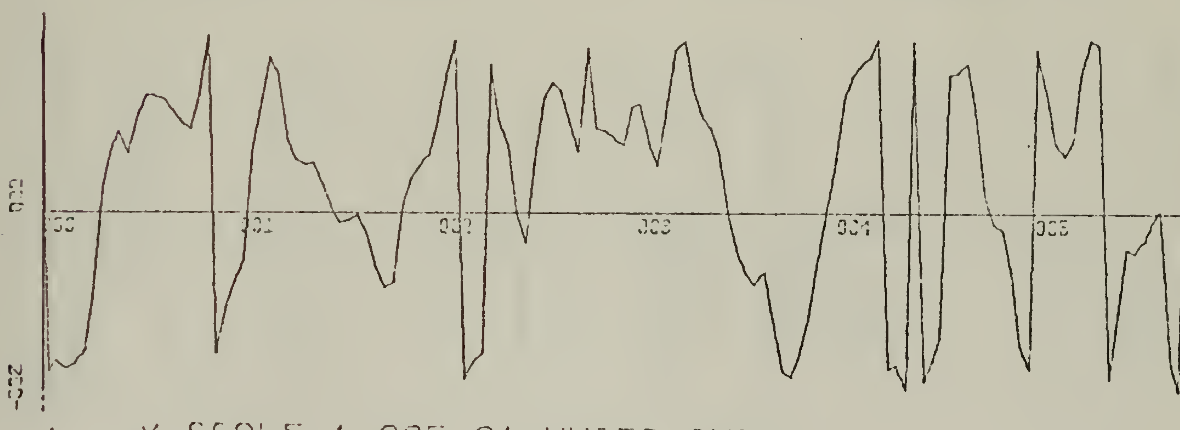

X-SCALE=1.00E-01 UNITS INCH.
Y-SCALE=2.00E+02 UNITS INCH.
PHASE SAL VS. W-PM RUN 6

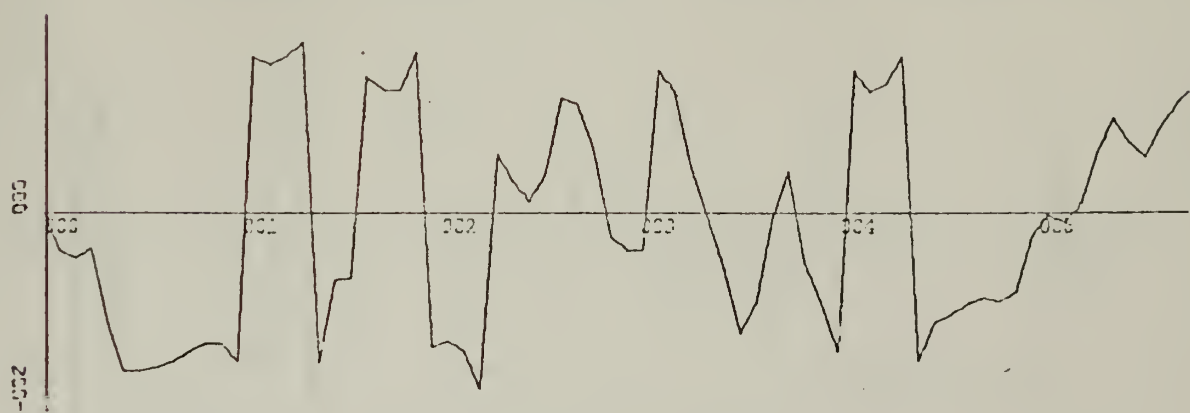

X-SCALE=1.00E-01 UNITS INCH.
Y-SCALE=2.00E+02 UNITS INCH.
PHASE SAL. VS. V-PM RUN 7

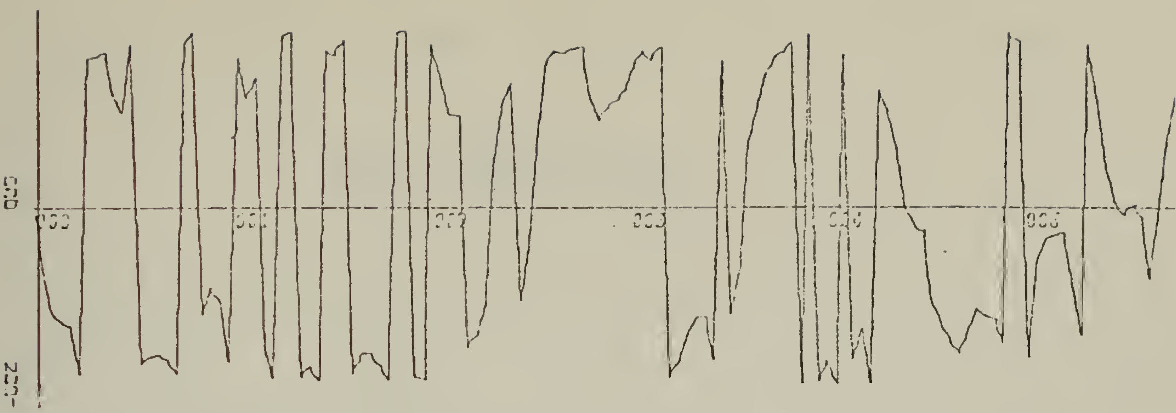

X-SCALE=1.00E-01 UNITS INCH.
Y-SCALE=2.00E+02 UNITS INCH.

PHASE SALL. VS. SSEL RUN 5

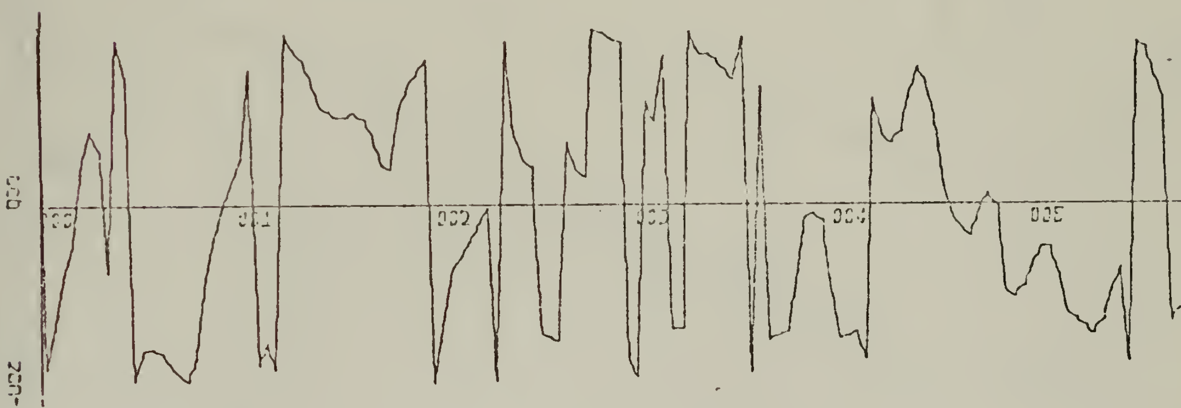

X-SCALE=1.00E-01 UNITS INCH.
Y-SCALE=2.00E+02 UNITS INCH.

PHASE SAL. VS. SSEL RUN 6

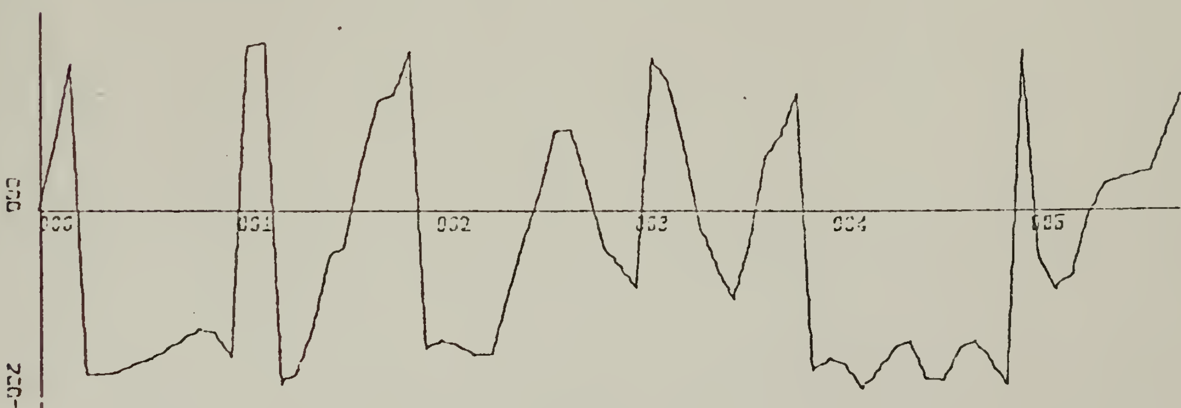

X-SCALE=1.00E-01 UNITS INCH.
Y-SCALE=2.00E+02 UNITS INCH.

PHASE SAL. VS. SSEL RUN 7

APPENDIX C
ENERGY DENSITY SPECTRA

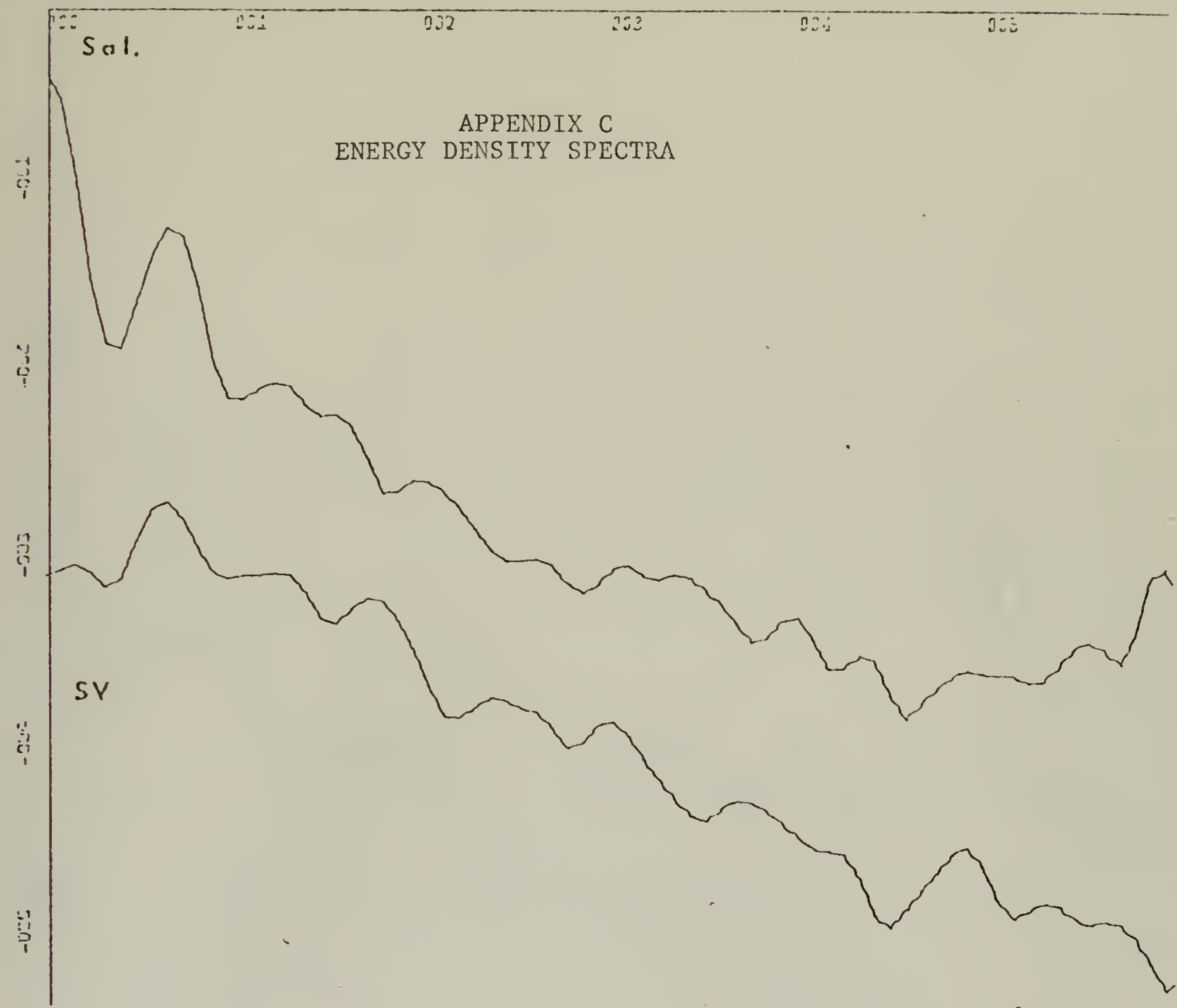

X-SCALE=1.00E-01 UNITS INCH.
Y-SCALE=1.00E+00 UNITS INCH.
ENERGY DENSITY-SAL. VS. SV. RUN 7

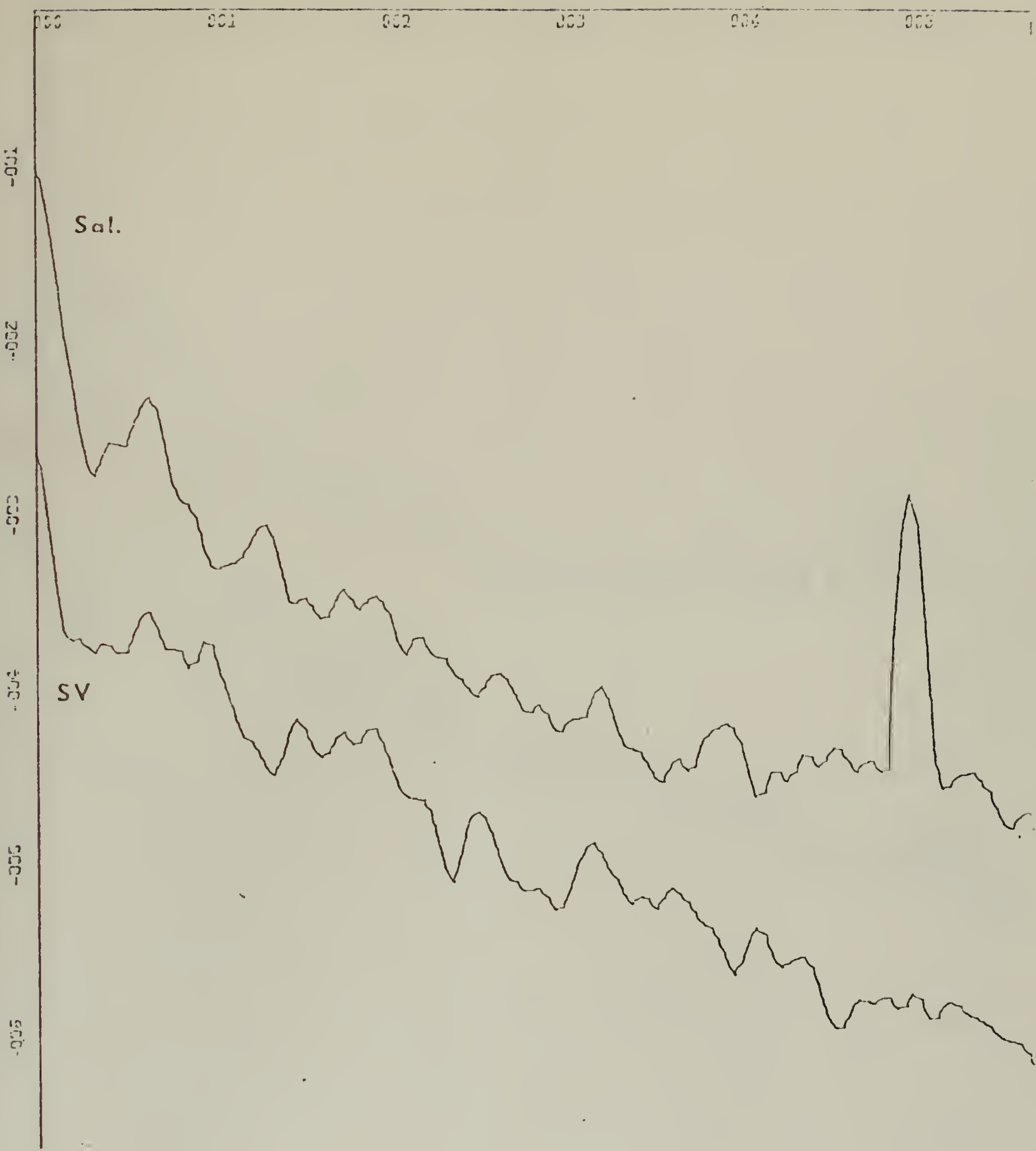

X-SCALE=1.00E-01 UNITS INCH.
Y-SCALE=1.00E+00 UNITS INCH.
ENERGY DENSITY-SAL. VS. SV. RUN 5

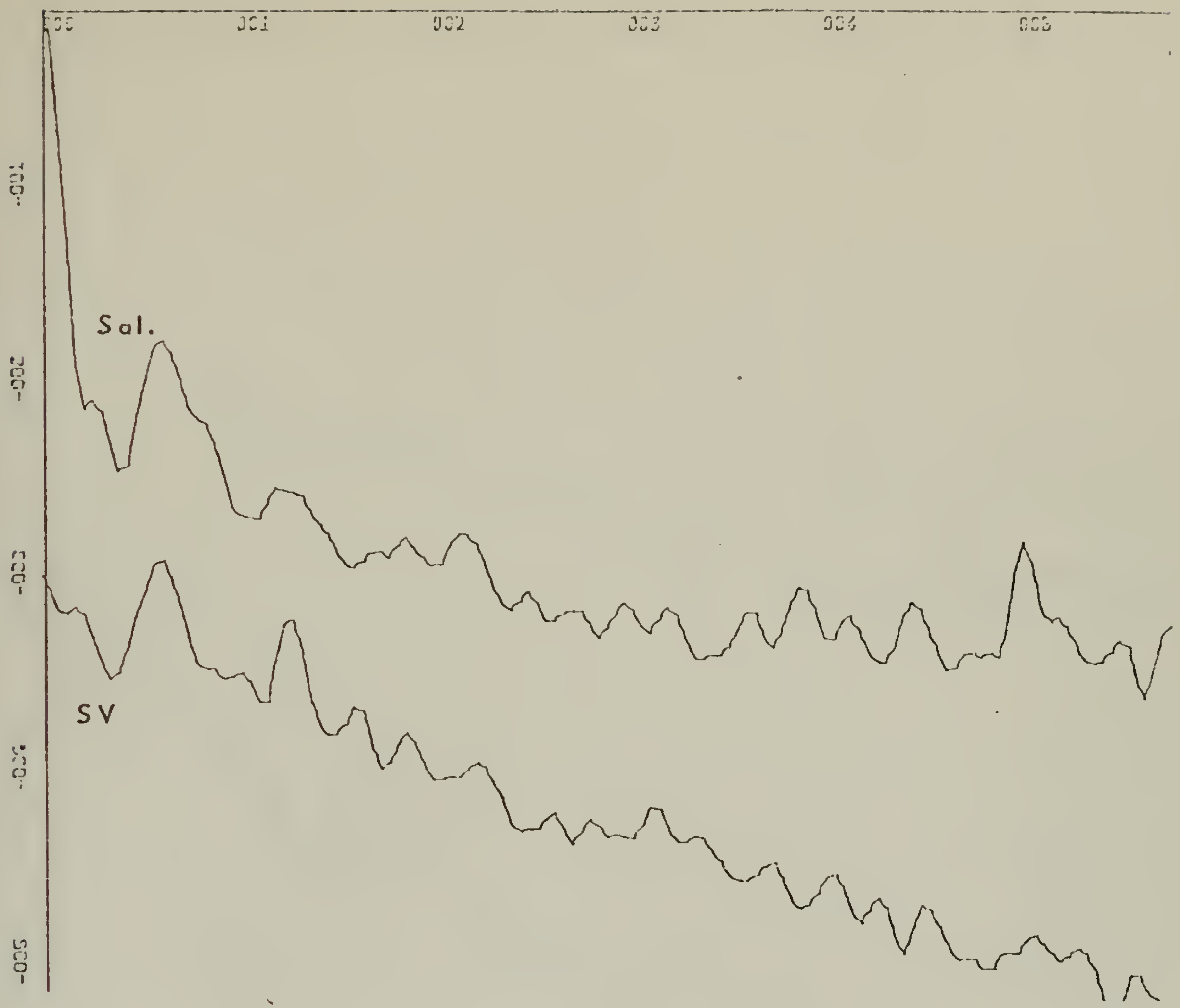

X-SCALE=1.00E-01 UNITS INCH.
Y-SCALE=1.00E+00 UNITS INCH.
ENERGY DENSITY-SAL. VS. SV. RUN 6

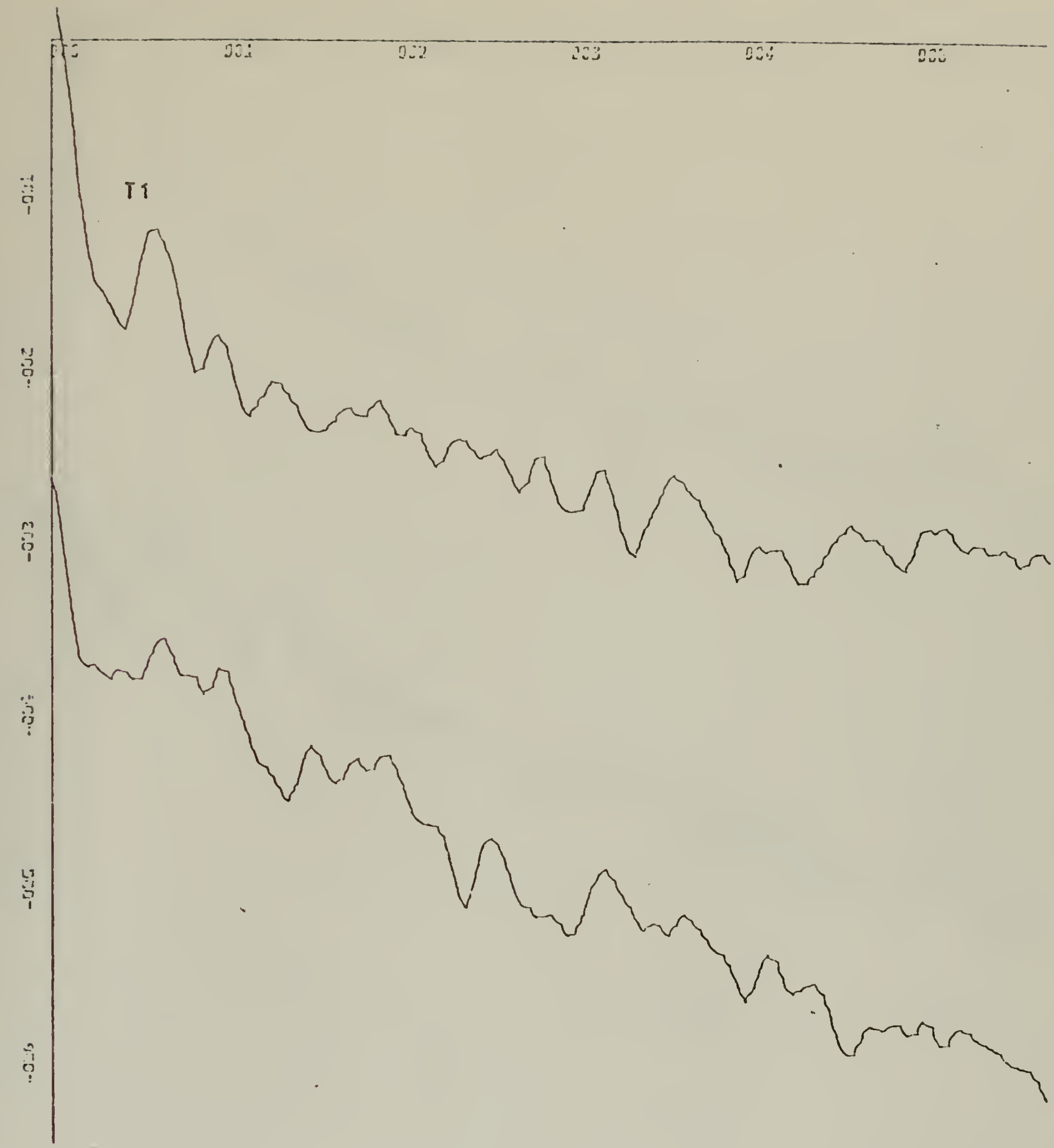

X-SCALE=1.00E-01 UNITS INCH.
Y-SCALE=1.00E+00 UNITS INCH.
ENERGY DENSITY SAL. VS. T1 RUN 5

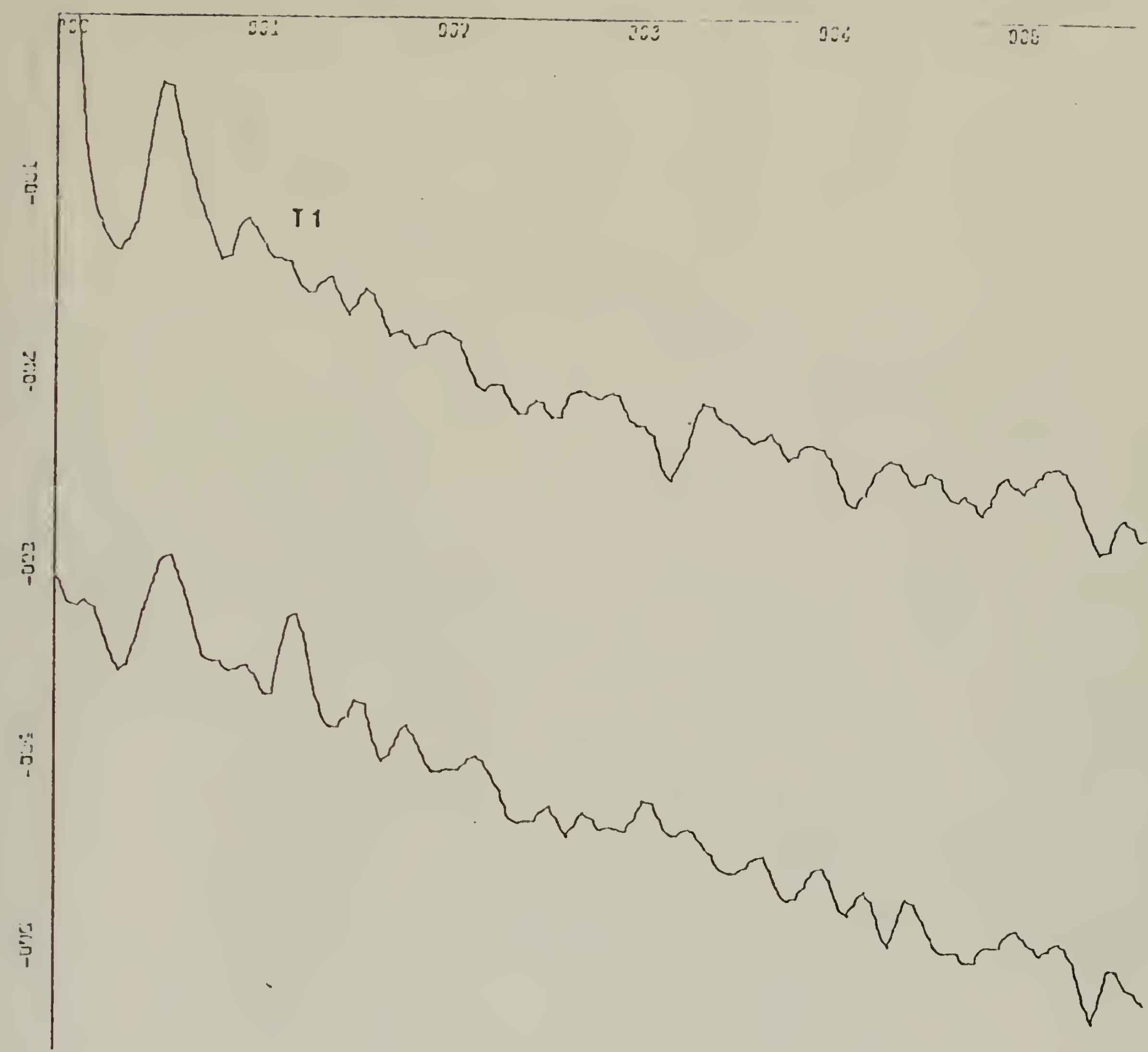

X-SCALE=1.00E-01 UNITS INCH.
Y-SCALE=1.00E+00 UNITS INCH.
ENERGY DENSITY SAL. VS. T1 RUN 6

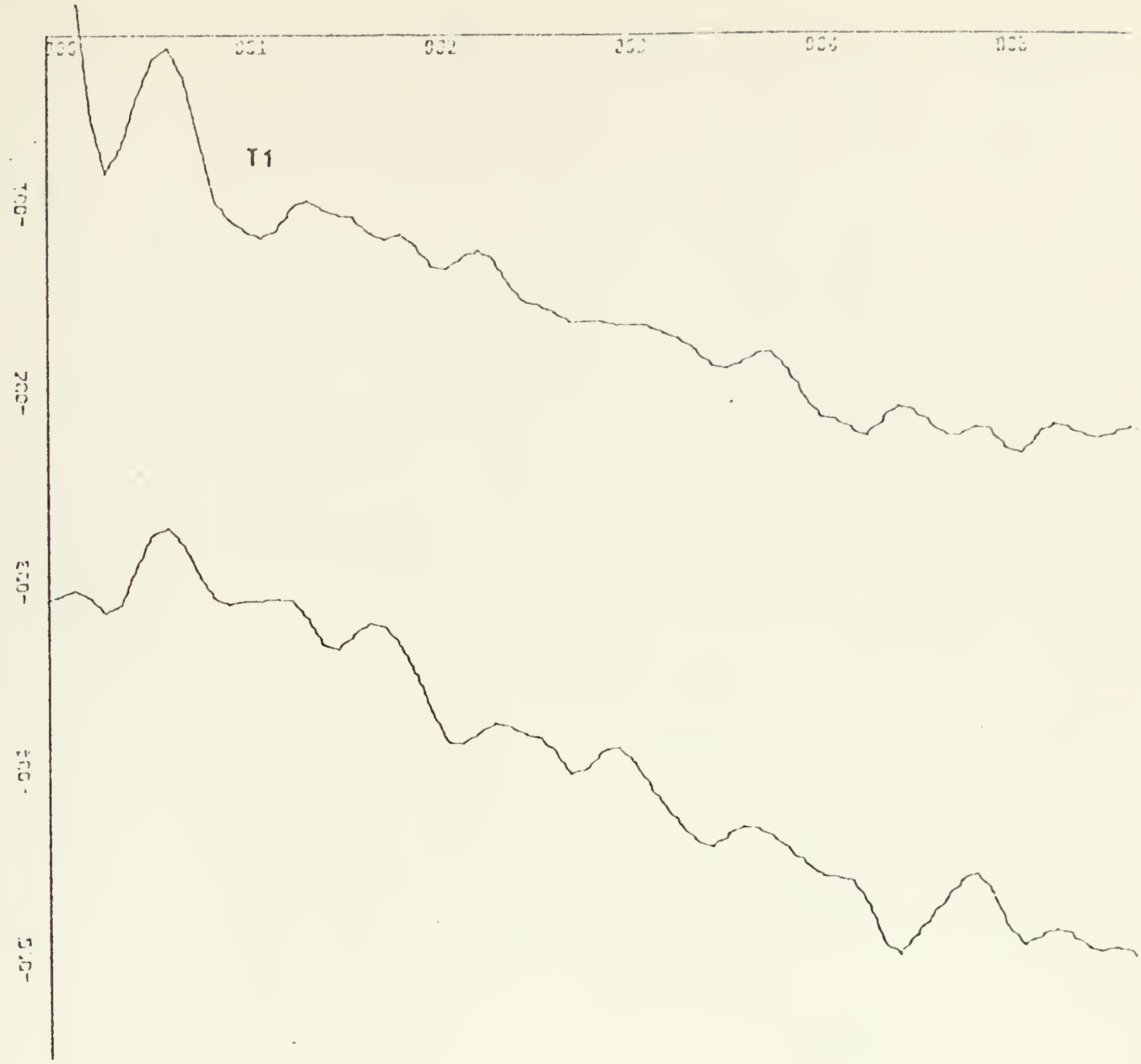

X-SCALE=1.00E-01 UNITS INCH.
Y-SCALE=1.00E+00 UNITS INCH.
ENERGY DENSITY SAL. VS. T1 RUN 7

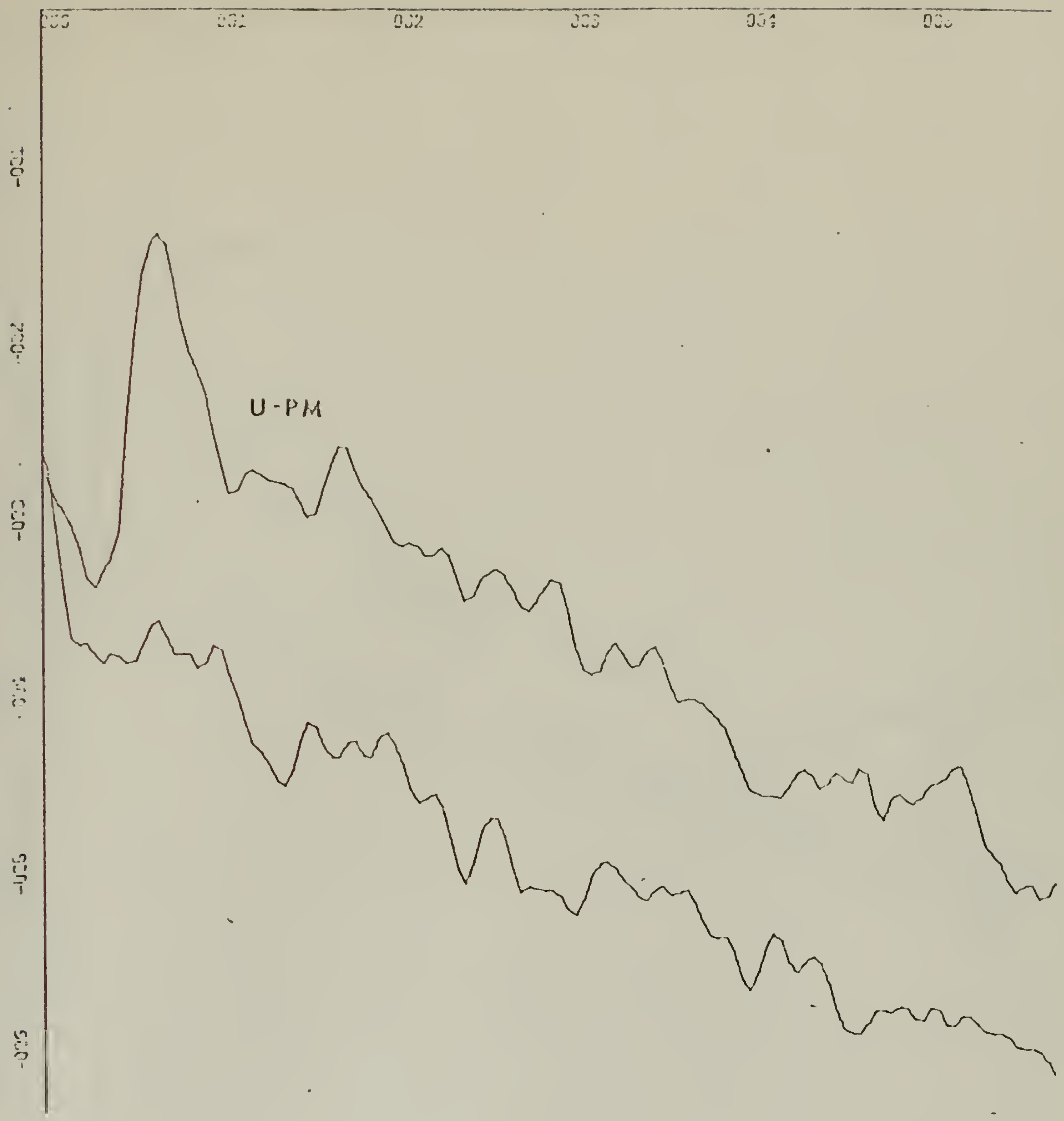

X-SCALE=1.00E-01 UNITS INCH.
Y-SCALE=1.00E+00 UNITS INCH.

ENERGY DENSITY SAL. VS. U-PM RUN 5

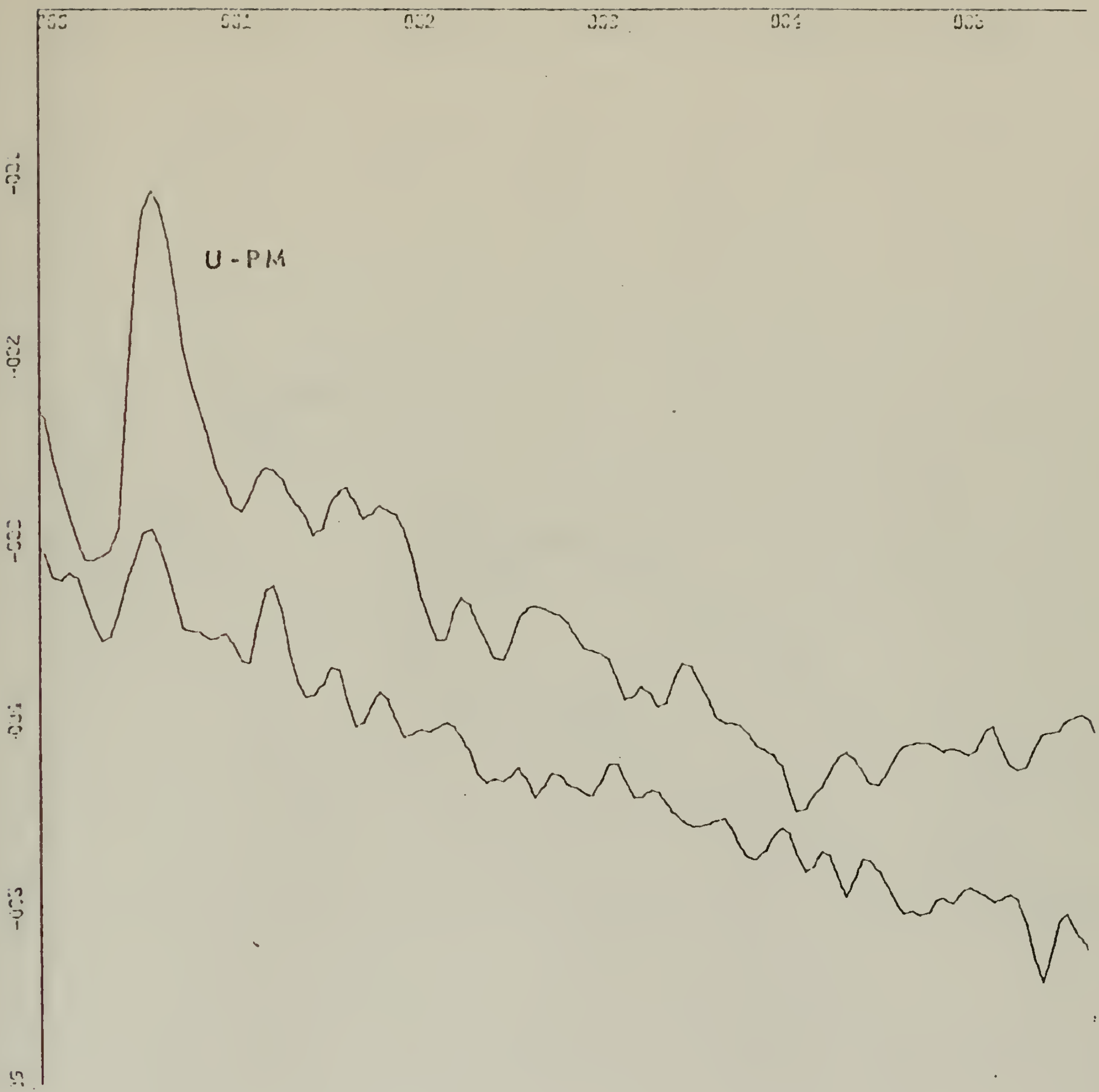

X-SCALE=1.00E-01 UNITS INCH.
Y-SCALE=1.00E+00 UNITS INCH.

ENERGY DENSITY SAL. VS. U-PM RUN 6

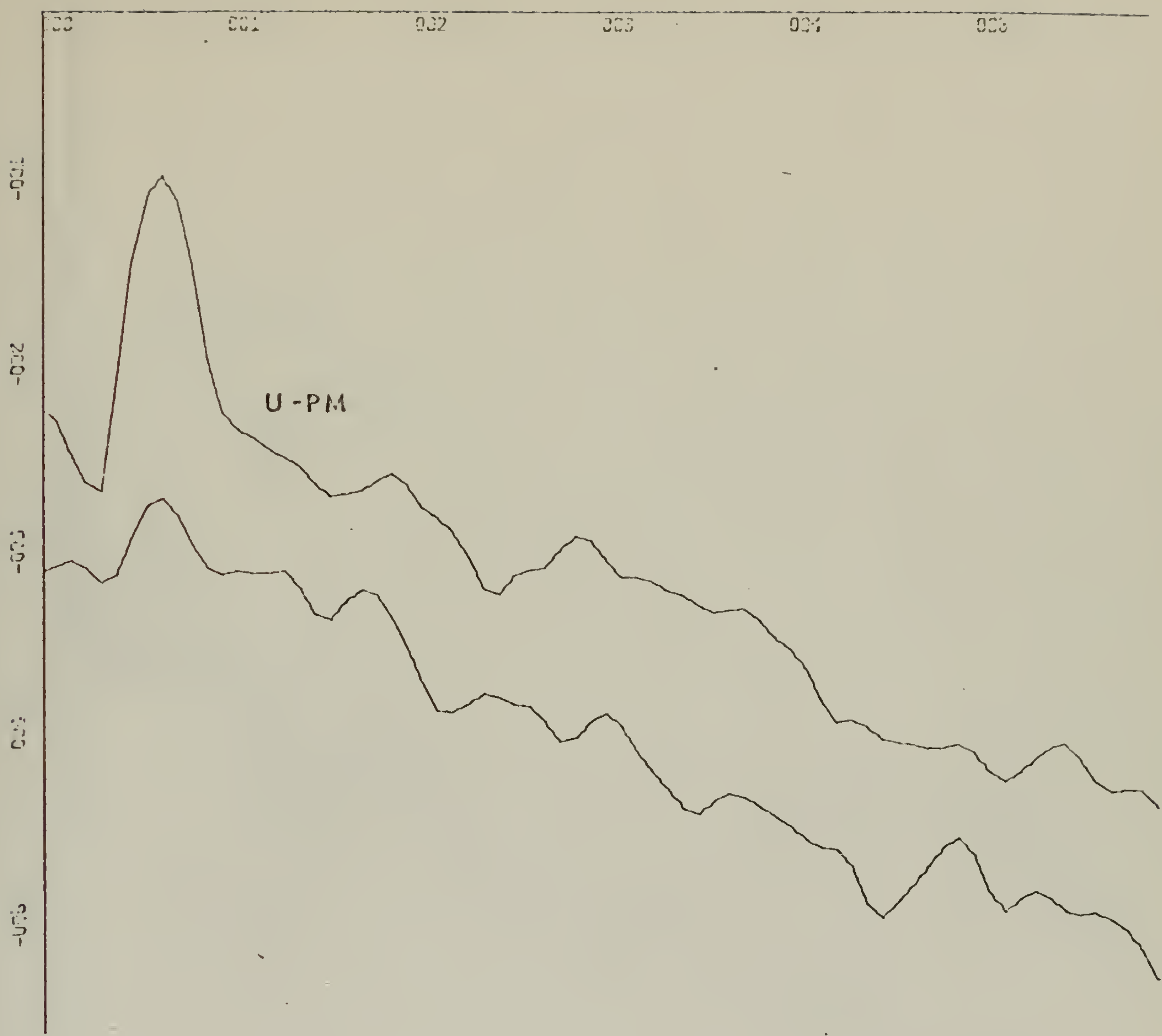

X-SCALE=1.00E-01 UNITS INCH.
Y-SCALE=1.00E+00 UNITS INCH.
ENERGY DENSITY SAL. VS. U-PM RUN 7

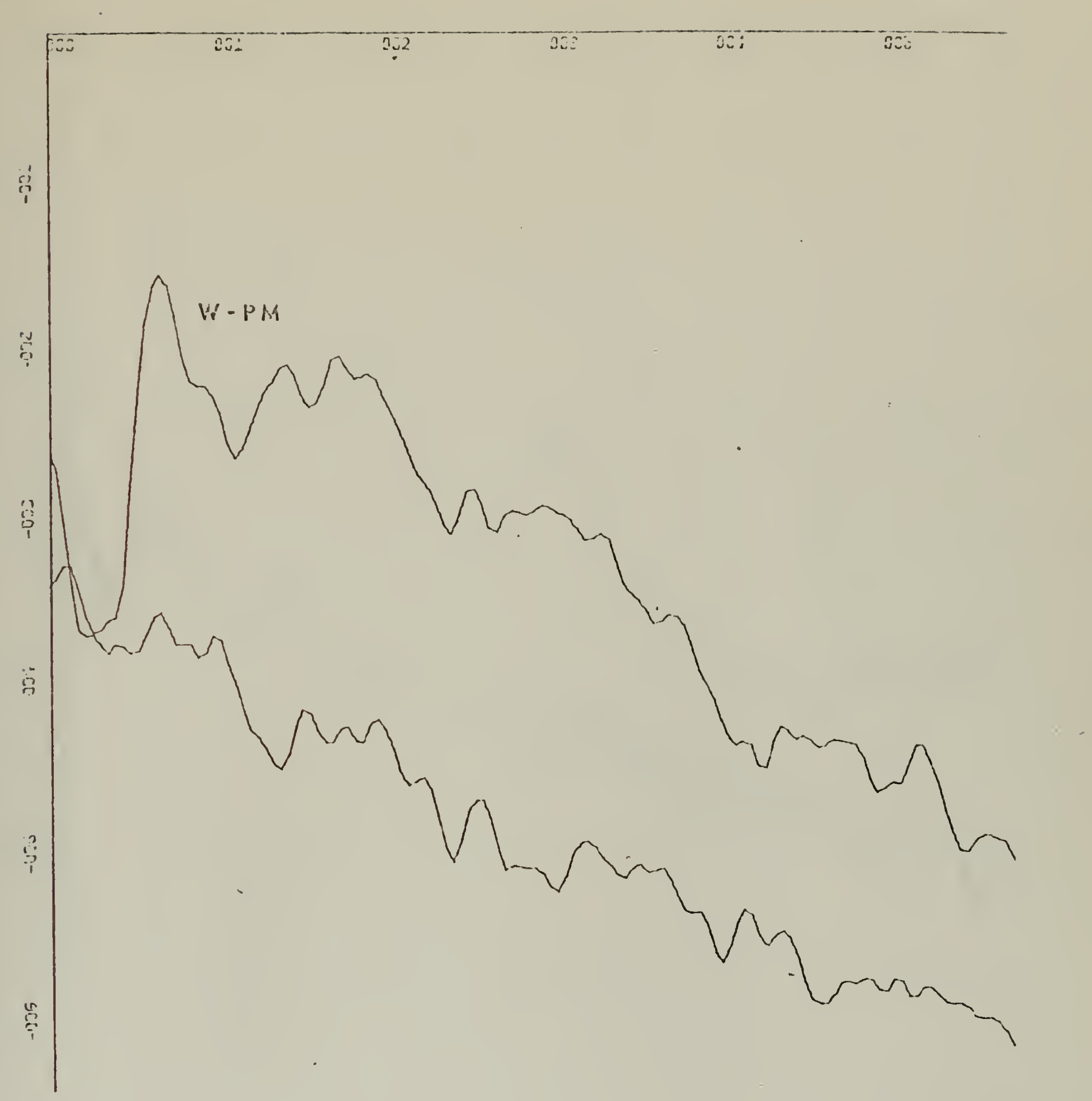

X-SCALE=1.00E-01 UNITS INCH.
Y-SCALE=1.00E+00 UNITS INCH.
ENERGY DENSITY SAL. VS. W-PM. RUN 5

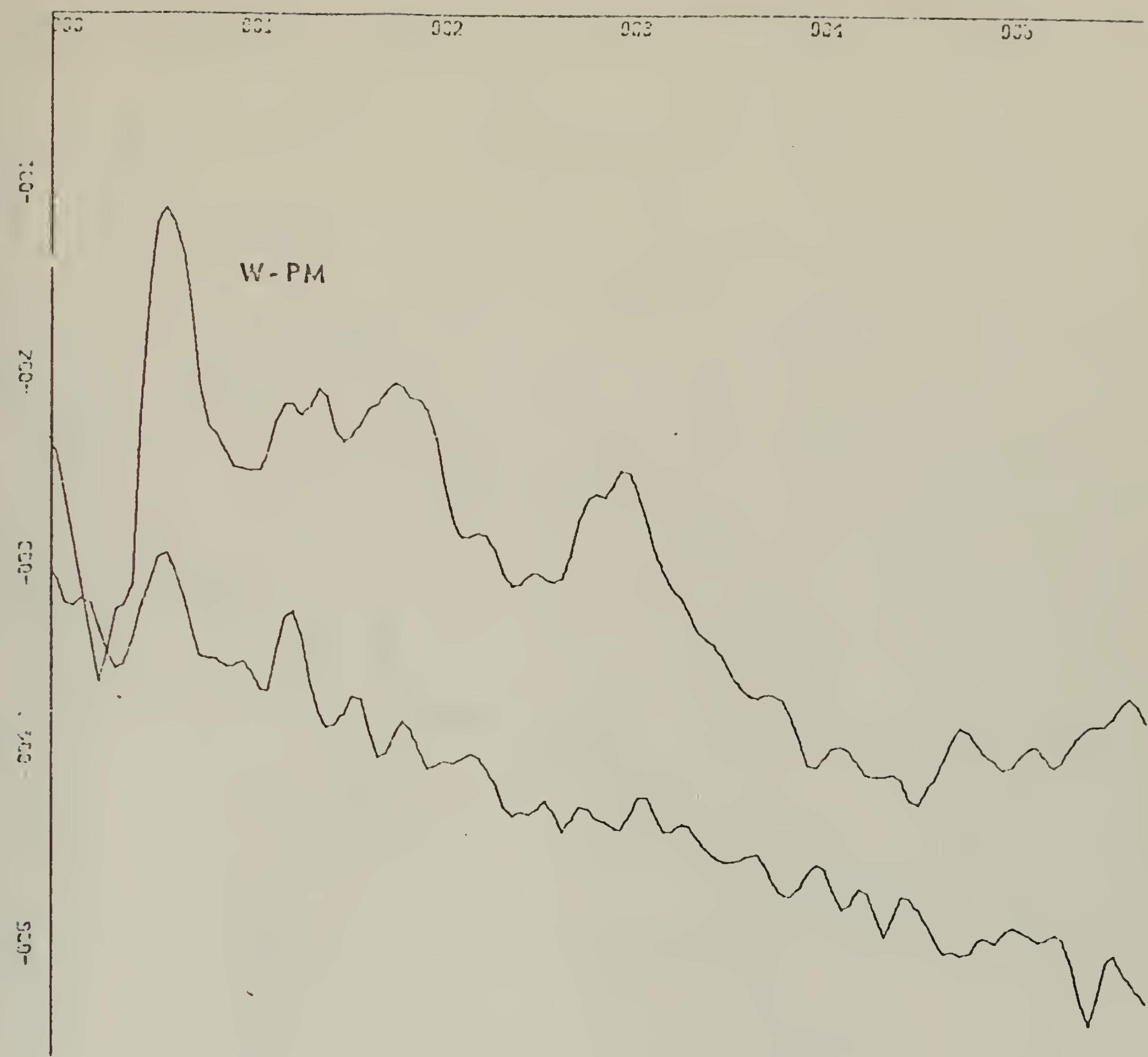

X-SCALE=1.00E-01 UNITS INCH.
Y-SCALE=1.00E+00 UNITS INCH.
ENERGY DENSITY SAL. VS. W-PM RUN 6

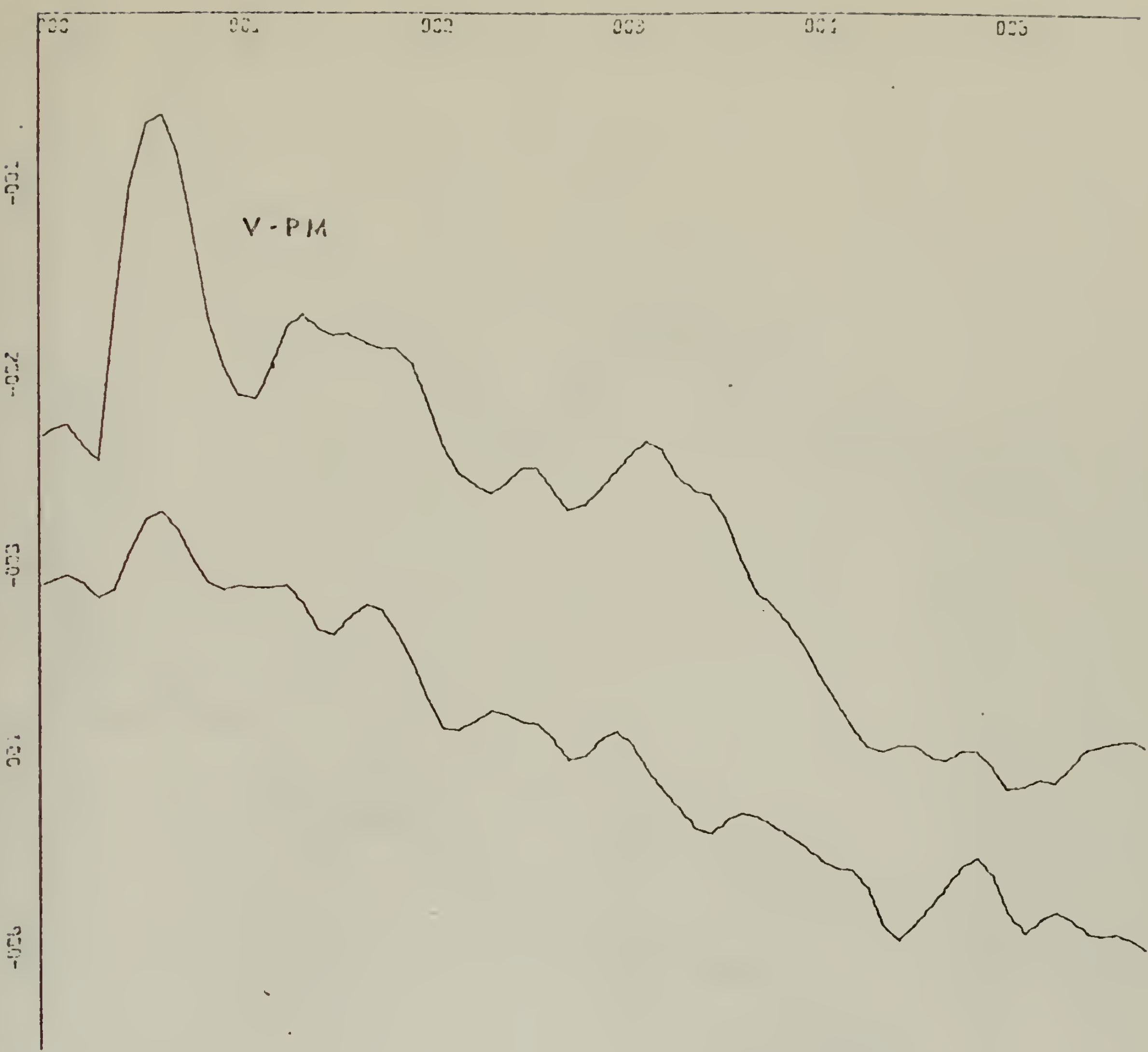

X-SCALE=1.00E-01 UNITS INCH.
Y-SCALE=1.00E+00 UNITS INCH.
ENERGY DENSITY SAL. VS. V-PM RUN 7

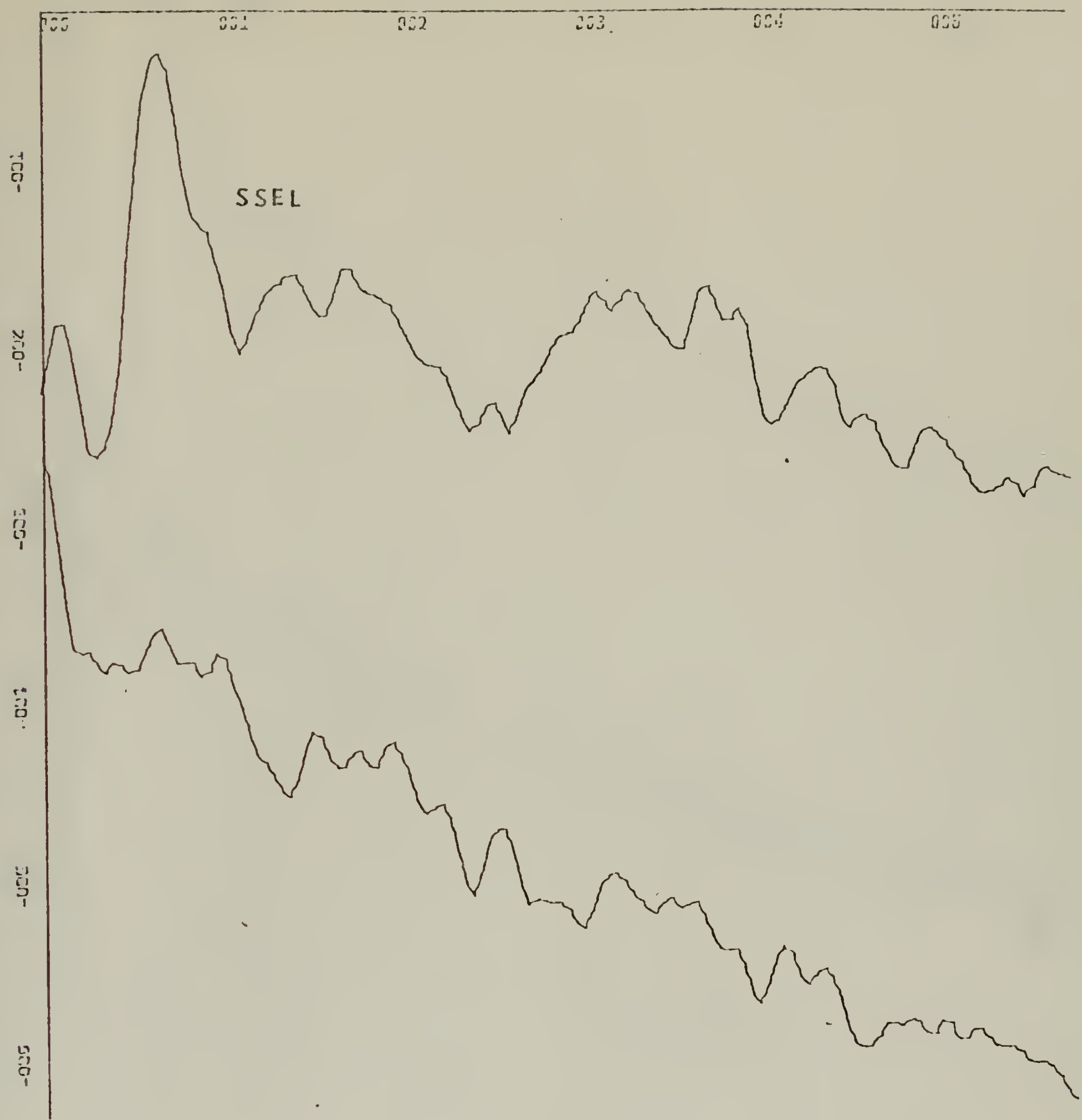

X-SCALE=1.00E-01 UNITS INCH.
Y-SCALE=1.00E+00 UNITS INCH.

ENERGY DENSITY SAL. VS. SSEL RUN 5

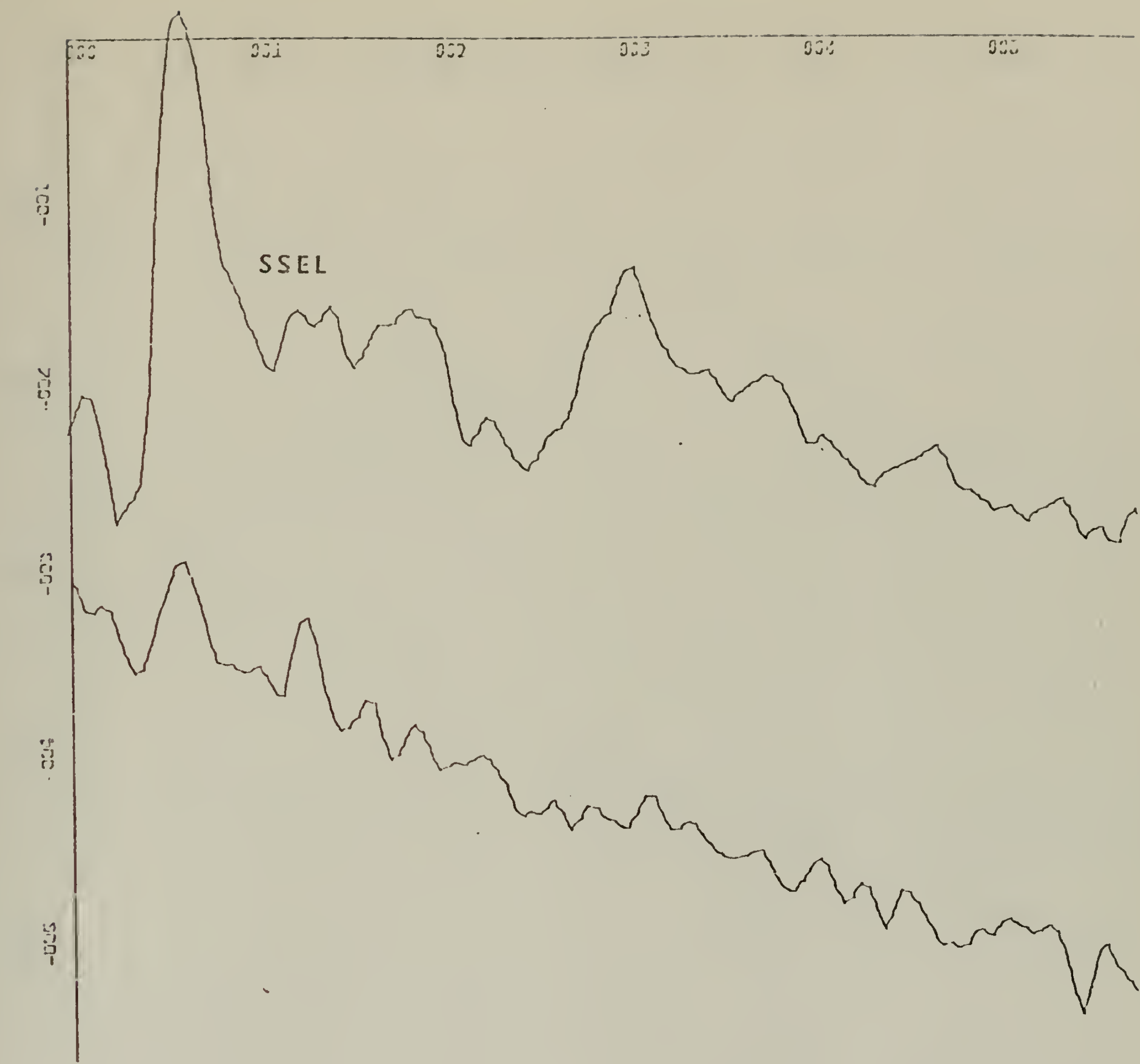

X-SCALE=1.00E-01 UNITS INCH.
Y-SCALE=1.00E+00 UNITS INCH.
ENERGY DENSITY SAL. VS. SSEL RUN 6

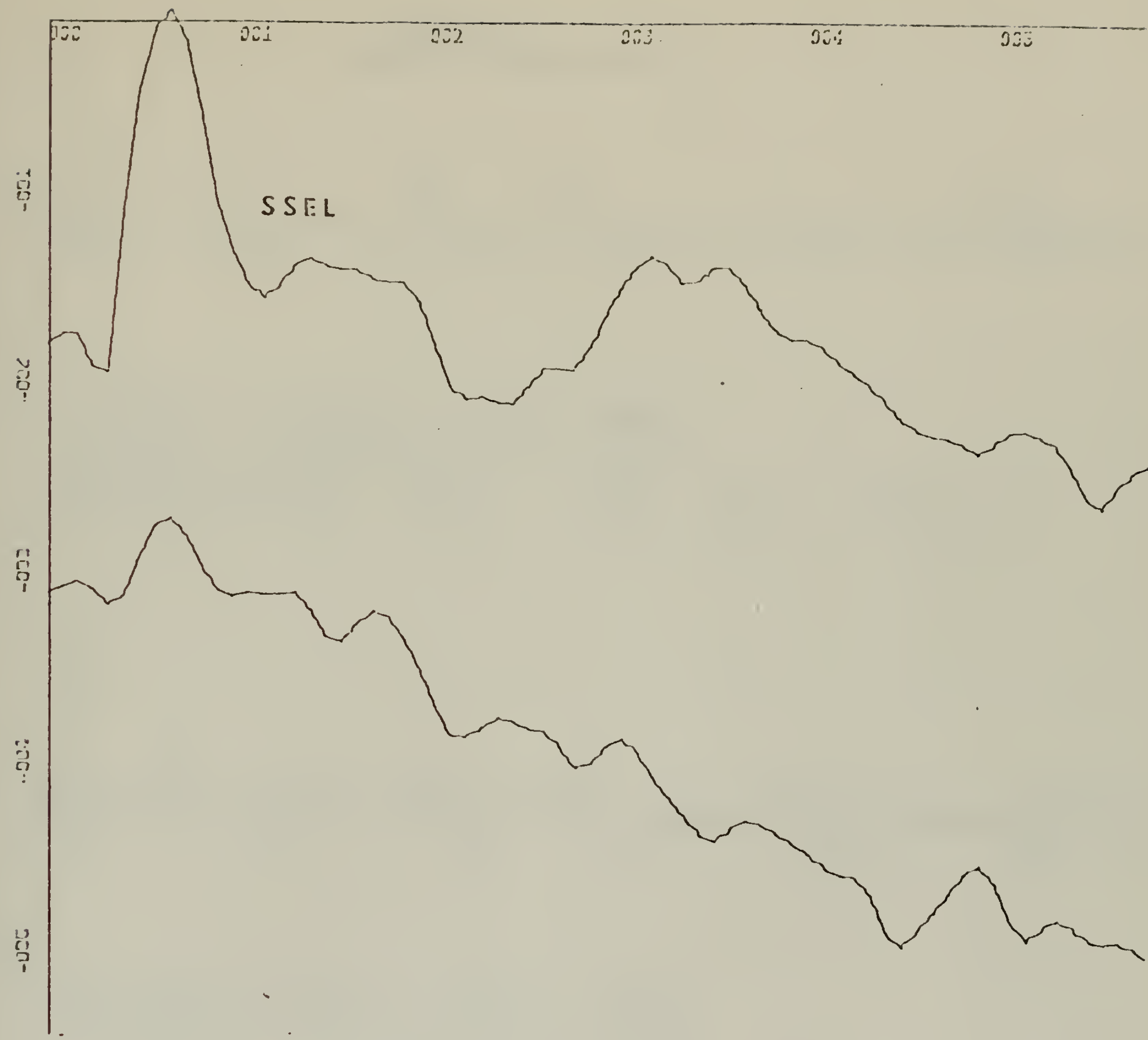

X-SCALE=1.00E-01 UNITS INCH.
Y-SCALE=1.00E+00 UNITS INCH.

ENERGY DENSITY SAL. VS. SSEL RUN 7

APPENDIX D
COHERENCE RELATIONSHIPS

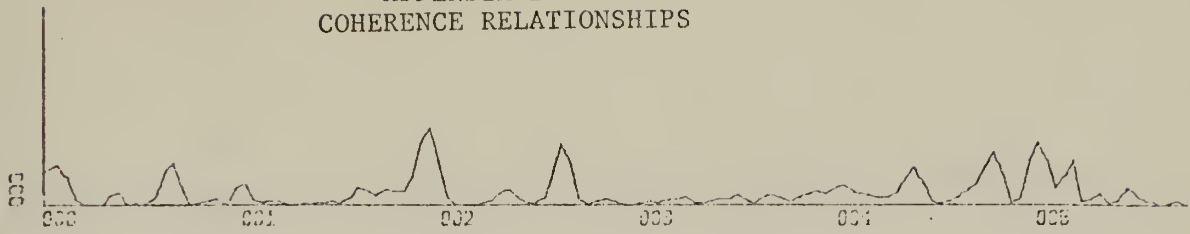

X-SCALE=1.00E-01 UNITS INCH.
Y-SCALE=1.00E+00 UNITS INCH.
COHERENCE-SAL. VS. SV. RUN 5

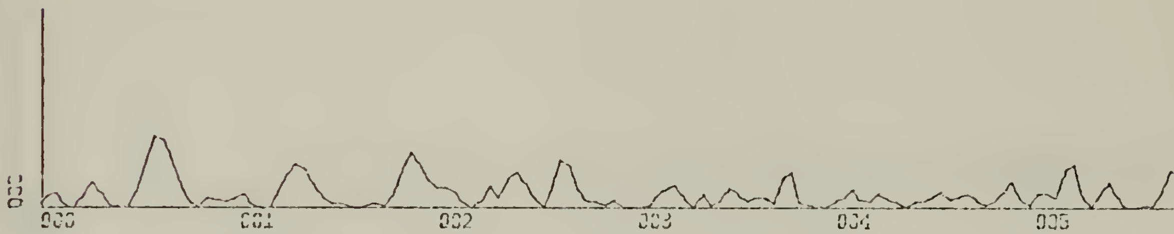

X-SCALE=1.00E-01 UNITS INCH.
Y-SCALE=1.00E+00 UNITS INCH.
COHERENCE-SAL. VS. SV. RUN 6

X-SCALE=1.00E-01 UNITS INCH.
Y-SCALE=1.00E+00 UNITS INCH.
COHERENCE-SAL. VS. SV. RUN 7

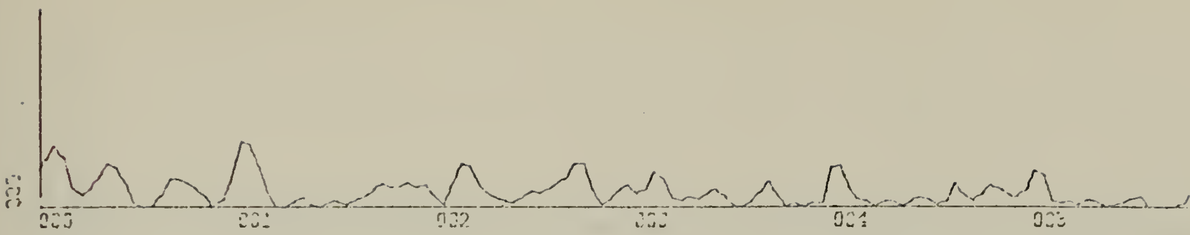

X-SCALE=1.00E-01 UNITS INCH.
Y-SCALE=1.00E+00 UNITS INCH.

COHERENCE SAL. VS. T1 RUN 5

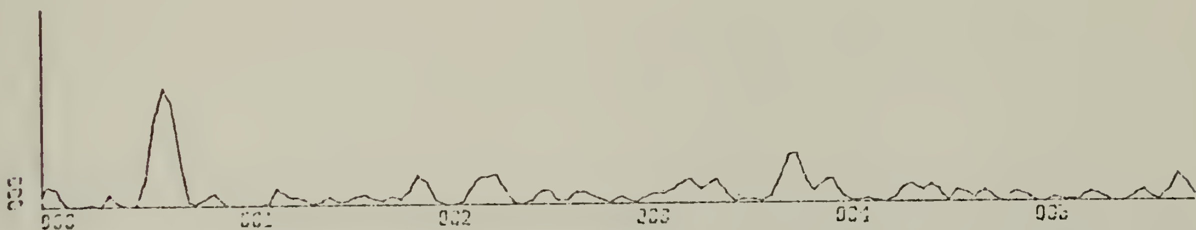

X-SCALE=1.00E-01 UNITS INCH.
Y-SCALE=1.00E+00 UNITS INCH.

COHERENCE SAL. VS. T1 RUN 6

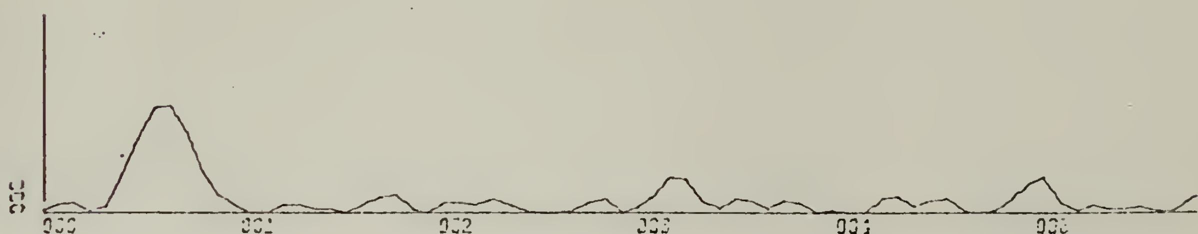

X-SCALE=1.00E-01 UNITS INCH.
Y-SCALE=1.00E+00 UNITS INCH.

COHERENCE SAL. VS. T1 RUN 7

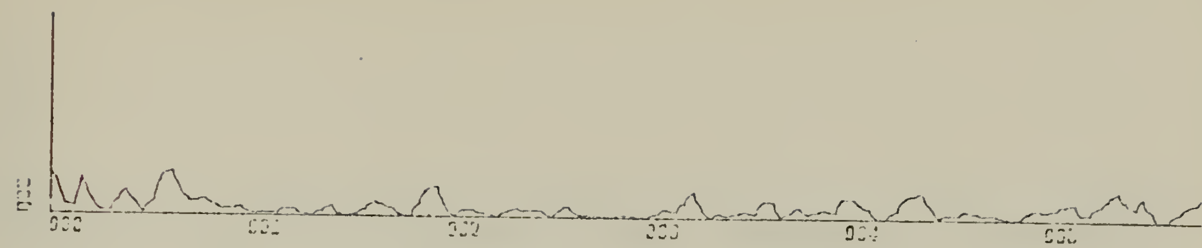

X-SCALE=1.00E-01 UNITS INCH.
Y-SCALE=1.00E+00 UNITS INCH.
CØHERENCE SAL. VS. U-PM RUN 5

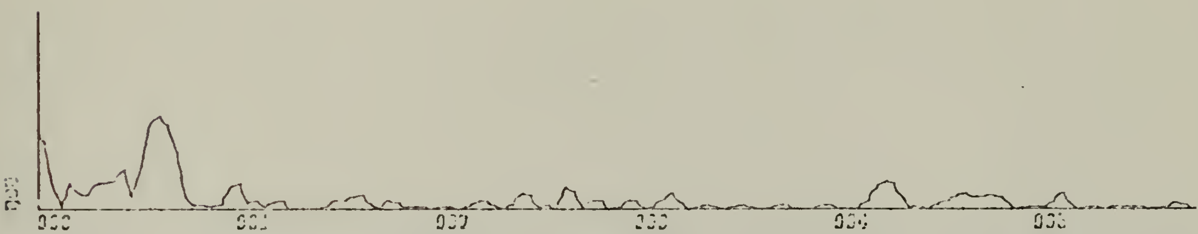

X-SCALE=1.00E-01 UNITS INCH.
Y-SCALE=1.00E+00 UNITS INCH.
CØHERENCE SAL. VS. U-PM RUN 6

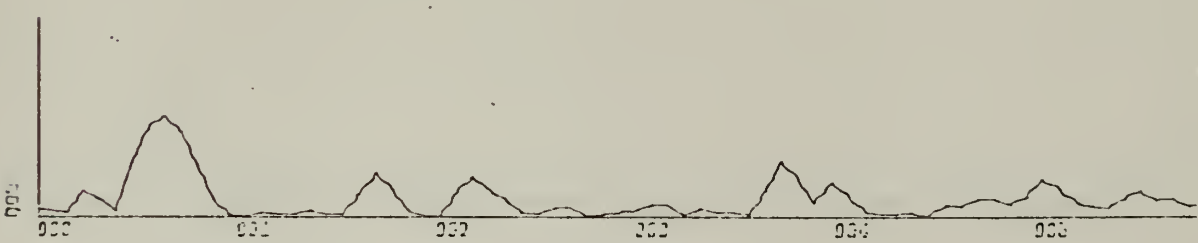

X-SCALE=1.00E-01 UNITS INCH.
Y-SCALE=1.00E+00 UNITS INCH.
CØHERENCE SAL. VS. U-PM RUN 7

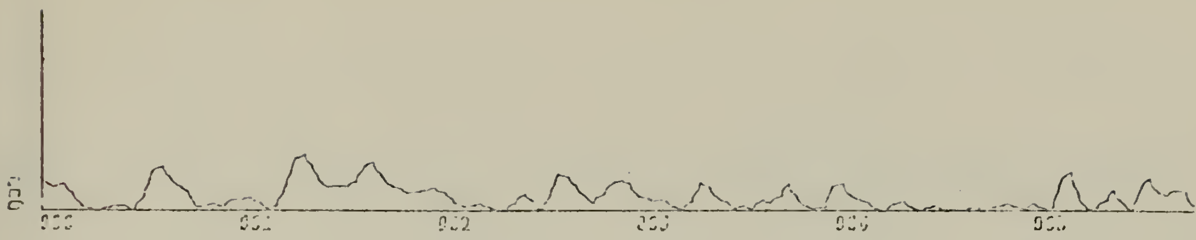

X-SCALE=1.00E-01 UNITS INCH.
Y-SCALE=1.00E+00 UNITS INCH.
COHERENCE SAL. VS. W-PM RUN 5

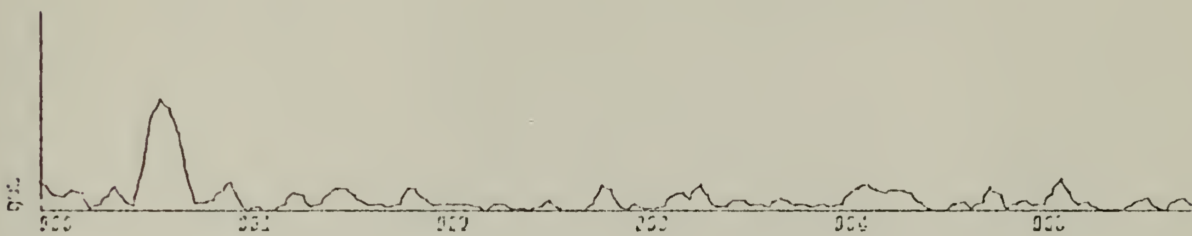

X-SCALE=1.00E-01 UNITS INCH.
Y-SCALE=1.00E+00 UNITS INCH.
COHERENCE SAL. VS. W-PM RUN 6

X-SCALE=1.00E-01 UNITS INCH.
Y-SCALE=1.00E+00 UNITS INCH.
COHERENCE SAL. VS. V-PM RUN 7

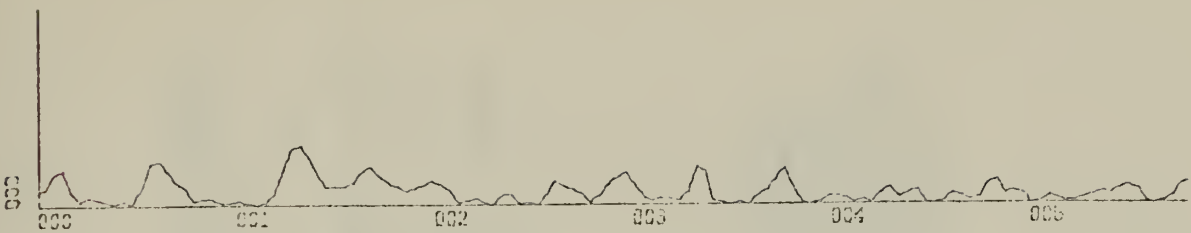

X-SCALE=1.00E-01 UNITS INCH.
Y-SCALE=1.00E+00 UNITS INCH.

COHERENCE SAL. VS. SSEL RUN 5

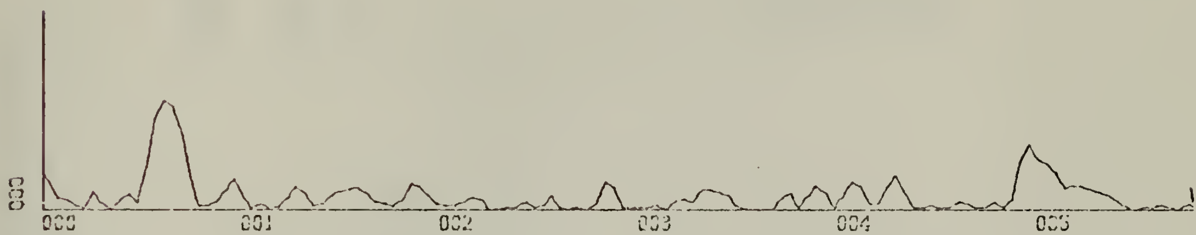

X-SCALE=1.00E-01 UNITS INCH.
Y-SCALE=1.00E+00 UNITS INCH.

COHERENCE SAL. VS. SSEL RUN 6

X-SCALE=1.00E-01 UNITS INCH.
Y-SCALE=1.00E+00 UNITS INCH.

COHERENCE SAL. VS. SSEL RUN 7

Salinity

vs.

Sound Velocity

Table V

Constant*	Run 5	Run 6	Run 7
NFLAG	1	1	1
NFLAGp	O	O	.O
ALAG	0.1	0.1	0.1
DT	0.2	0.2	0.2

*Constant inputs to program. These are defined on comment cards on the following page.

Table VI

Input*	Run 5	Run 6	Run 7
CALX1	2.0	2.0	2.0
CALX2	0.1019	0.1019	0.1019
JF	3072	3072	3072
JF1	3068	3068	3068
NREC	12	12	7
LCH 1	2	2	2
LCH 2	1	1	1

*Variable inputs to program. These are defined on comment cards on the following page. In this example, CALX1 factor pertains to sound velocity and CALX 2 pertains to salinity.

```
C     PRCGRAM FOR THE SPECTRAL ANALYSIS OF APERIODIC RECORDS
C     DATA MUST BE SAMPLED AT EQUAL INTERVALS CF DT
C     CALCULATES EITHER THE AUTO SPECTRA OR THE CROSSSPECTRA
C     IF NFLAG1=0 , AUTOSPECTRA.........IF NFLAG1=1    COSPECTRA
C     IF NFLAGP = 1 ...... CALL PRESS, TOTE
C NTS= NUMBER OF TIME SAMPLES
C ALAG=PERCENT OF TIME LAG
C DT = TIME INCREMENT
C DHZ = FREQUECY SPACING
C DHZ = 1/(2*TM)
C TM =DT*MLAG
C FBHZ = LOWEST FREQUENCY (HZ)
C FBHZ = 1/(2*TM) 1/(2*MLAG*DT)
C FEHZ = HIGHEST FREQUENCY OF INTEREST (HZ)
C FEHZ = NIQUEST FREQUENCY = 1/(2*DT)
C TRANS-- INSTRUMENT AND REMARKS
C     CALX1-- CALIBRATION FACTOR FOR ANALOG TO DIGITAL CONVERSION
C     CALX2-- CALIBRATION FACTOR FOR ANALOG TO DIGITAL CONVERSION
C     JF--NUMBER OF DATA BITS  CONTAINED IN RUN
C     JF1--NUMBER OF  DATA BITS CONTAINED IN RUN
C     NREC--NUMBER OF RECORDS CONTAINED IN RUN
C     LCH1--POSITION OF RECORD BY TRACK SEQUENCE NUMBER
C     LCH2--POSITION OF RECCRD BY TRACK SEQUENCE NUMBER
      REAL*8 ITITEL(12),ITITIL(12),ITITLI(12),ITITLL(12)
      DIMENSION DIFF(748)
      DIMENSION WSPE(748)
      DIMENSION F1(6500),F2(6500),FILE1(3072)
      DIMENSION PHI(950),TAU(950),SPHI(748),APHI(748),PHN(748),PHN1(748)
      DIMENSION FREQ(748),CYCL(748),SPEC(748),SSP(748),WSPEC(748)
      DIMENSION CSPEC(748),QSPEC(748),SS2(748),PHN2(1496)
      DIMENSION RESPF(748),PER(748),SPE2(748),PHASE(748),COHER(748)
      DIMENSION XK(748)
      DIMENSION DATE(2),HCUR(2),TRANS(10)
      REAL*4 LABE1/'  F1'/,LABE2/'  F2'/,LABEL5/'PHAS'/,LABEL6/'COHE'/,L
     1ABEL7/'  F2'/,LABEL8/'  F1'/
  530 READ(5,200,END=999)(ITITEL(I),I=1,12)
      READ(5,200) (ITITIL(I),I=1,12)
      READ(5,200) (ITITLI(I),I=1,12)
      READ (5,200) (ITITLL(I),I=1,12)
  200 FORMAT(6A8)
      READ(5,802) DATE,HOUR,TRANS
  802 FORMAT(2A4,2A4,10A4)
      READ(5,96) NFLAG1,NFLAGP
   96 FORMAT (3I6)
      READ(5,99) NTS,ALAG,DT,DHZ,FBHZ,FEHZ
   99 FORMAT(I6,F6.0,5F10.0)
      READ(5,801) CALX1,CALX2,H,X2
      J=1
```

```
      READ(5,1000)JF,JF1,NREC,LCH1,LCH2
  500 READ(4,1005,END=520)(FILE1(I),I=1,JF)
      DO 510 JK=LCH1,JF1,6
      F1(J)=FILE1(JK)
      F2(J)=FILE1(JK+LCH2)
      J=J+1
  510 CONTINUE
      GO TO 500
  520 NTS=(NREC-1)*512
      MLAG=ALAG*NTS
      DHZ=1.0/(2.0*DT*MLAG)
      FEHZ=1.0/(2.0*DT)
 1000 FORMAT(5I5)
 1005 FORMAT(24(128A4))
      WRITE(6,811)
  811 FORMAT(1H1)
      WRITE(6,803) DATE,HOUR,TRANS
      WRITE(6,98) NTS,MLAG,DT,DHZ,FBHZ,FEHZ,CALX1,CALX2,H,X2
   98 FORMAT(7H NTS = ,I6//,8H MLAG = ,I6//,6H DT = ,F9.5//,6H DHZ= ,F10
     1.8//,' FBHZ = ',F10.8//,' FEHZ = ',F12.8//,' CALX1 = ',F10.8//,
     2' CALX2 = ',F10.8//,' H = ',F10.3//,' X2 = ',F10.3//)
  801 FORMAT(6F10.5)
  803 FORMAT(40H UPPER OCEAN TURBULENCE STUDY              ,5X,7H DATE  ,2A
     14,10H   HOUR    ,2A4//,5X,10A4///)
C BAND WIDTH FREQUENCIES OF TOTAL ENERGY FLUX- CMIN,CMAX
      CMIN=0.0
      CMAX=2.5
C COMPUTING POWER SPECTRUM
      PI=3.14159265
      FB = FBHZ*2.0*PI
      FE = FEHZ*2.0*PI
      DF = DHZ *2.0*PI
      FMIN = 2.0*PI*CMIN
      FMAX = 2.0*PI*CMAX
      WRITE(6,901)(F1(I),I=1,NTS)
  901 FORMAT (' ',18F7.3)
      CALL TREND(F1,NTS,DT,CALX1)
   21 DO 10 M=1,MLAG
      SUM=0.0
      NMAX=NTS-M+1
      DO 8 I=1,NMAX
      NN=M+I-1
    8 SUM=SUM+F1(I)*F1(NN)
      XNMAX=NMAX
      XX=M-1
      TAU(M)=XX*DT
      PHI(M)=SUM/XNMAX
      PHN(M) = PHI(M)/PHI(1)
```

```
   10 CONTINUE
      CALL PARZ(MLAG,PHI)
  798 FORMAT(' PHI(0) = ',F10.6//)
      NFREQ=(FE-FB)/DF+0.1
      DO 14 N=1,NFREQ
      XN=N
      FREQ(N)=(XN-1.0)*DF+FB
   14 CYCL(N) = FREQ(N)/(2.0*PI)
      PER(1) = 0.0
      DO 15 N = 2,NFREC
   15 PER(N) = 1.0/CYCL(N)
      MLAGM1=MLAG-1
      XMLAG=MLAG
   46 DO 50 N=1,NFREQ
      SUM=0.5*(PHI(1)+PHI(MLAG)*COS(FREQ(N)*TAU(MLAG)))
      C1=COS(FREC(N)*DT)
      S1=SIN(FREQ(N)*DT)
      CC=1.0
      SC=0.0
      DO 49 M=2,MLAGM1
      CT=CC*C1-SC*S1
      ST=SC*C1+CC*S1
      CC=CT
      SC=ST
   49 SUM=SUM+PHI(M)*CC
   50 SPEC(N)=SUM*2.0/XMLAG
C     SPECTRAL VALUES -- A*A/DHZ*DHZ ( AMPLITUDE SQUARED/HZ)
      IF(NFLAGP) 741,741,742
  742 CONTINUE
      CALL PRESS(FREQ,SPEC,WSPEC,NFREQ,RESPF,XK,H,X2,DF,FB,FMAX)
  741 CONTINUE
C SUBROUTINE TO CALCULATE VARIANCE
      SUM = 0.0
      DO 650 N=1,NFREQ
  650 SUM = SUM + SPEC(N)
      WRITE(6,651) SUM
  651 FORMAT (25H     VARIANCE OF SPECTRUM//,3X,16H     VARIANCE = ,F10.
     17,10H   M2     //)
      WRITE(6,798) PHI(1)
      CALL AVER(F1,NTS,DF)
      IF(NFLAG1) 743,743,744
  744 CONTINUE
C CCMPUTING CROSS-CORRELATION FUNCTION
      WRITE(6,806)
  806 FORMAT('0',19H WAVE RECORD NO.  4//)
      WRITE(6,901)(F2(I),I=1,NTS)
      CALL TREND(F2,NTS,CT,CALX2)
      CALL AVER(F2,NTS,DT)
```

```
      DO 70 M=1,MLAG
      SUM=0.0
      NMAX=NTS-M+1
      DO 7 I=1,NMAX
      NN=M+I-1
    7 SUM=SUM+F2(I)*F2(NN)
      XNMAX=NMAX
      XX=M-1
      TAU(M)=XX*DT
      PHI(M)=SUM/XNMAX
      PHN1(M) = PHI(M)/PHI(1)
   70 CONTINUE
      WRITE(6,112)
      WRITE(6,107)(TAU(M),PHN(M),PHN1(M),M=1,MLAG)
      CALL DRAW(480,TAU,  PHN,1,0,LABE1,ITITEL,00.0,0.0,2,0,2,0,6,8,1,
     1LAST)
      CALL DRAW(480,TAU, PHN1,3,0,LABE2,ITITEL,00.0,0.0,2,0,2,0,6,8,1,
     1LAST)
      CALL PARZ(MLAG,PHI)
      DO 71 N=1,NFREQ
      SUM=0.5*(PHI(1)+PHI(MLAG)*COS(FREQ(N)*TAU(MLAG)))
      C1=COS(FREQ(N)*DT)
      S1=SIN(FREQ(N)*DT)
      CC=1.0
      SC=0.0
      DO 79 M=2,MLAGM1
      CT=CC*C1-SC*S1
      ST=SC*C1+CC*S1
      CC=CT
      SC=ST
   79 SUM=SUM+PHI(M)*CC
   71 SPE2(N)=SUM*2.0/XMLAG
      IF(NFLAGP) 73,73,72
   72 CONTINUE
   73 CONTINUE
   20 MMT=2*MLAG-1
      DO 5 M=1,MMT
      AB=M-MLAG
      MAB=ABS(AB)
      IT=NTS-MAB
      IF(M-MLAG) 1,1,2
    1 IB1=MLAG-M+1
      IB2=1
      GO TO 3
    2 IB1=1
      IB2=M-MLAG+1
    3 SUM=0.0
      DO 4 I=1,IT
```

```
      I1=IB1+I-1
      I2=IB2+I-1
    4 SUM=SUM+F1(I1)*F2(I2)
      XIT=IT
      PHI(M)=SUM/XIT
      PHN2(M) = PHI(M)/PHI(1)
      TAU(M)=M-MLAG
    5 TAU(M)=TAU(M)*DT
C     PARZEN FILTER APPLIED TO CORRELLATION FUNCTION
      XMLAG = MLAG
      MLAGH = XMLAG/2.0-0.1
      MLAGH1 = MLAGH + 1
      DC 31 M=1,MLAGH
      MM = M-1
      R = MM
      RM = R/XMLAG
      MA = MLAG+ MM
      MB = MLAG - MM
      UM = 1.0-6.0*RM*RM*(1.0-RM)
      PHI(MA) = PHI(MA)*UM
      PHI(MB) = PHI(MB)*UM
   31 CCNTINUE
      DO 32 M = MLAGH1,MLAG
      MM = M-1
      R = MM
      RM = R/XMLAG
      RM1 = (1.0-RM)
      MA = MLAG+ MM
      MB = MLAG - MM
      UM = 2.0*RM1*RM1*RM1
      PHI(MA) = PHI(MA)*UM
      PHI(MB) = PHI(MB)*UM
   32 CCNTINUE
   28 DO 30 M=1,MLAG
      MM=M-1
      MA=MLAG+MM
      MB=MLAG-MM
      SPHI(M)=PHI(MA)+PHI(MB)
   30 APHI(M)=PHI(MA)-PHI(MB)
      DC 40 N=1,NFREQ
      SUM1=0.5*(SPHI(1)+SPHI(MLAG)*COS(FREQ(N)*TAU(MLAG)))
      SUM2=0.5*(APHI(1)+APHI(MLAG)*SIN(FREQ(N)*TAU(MLAG)))
      C1=COS(FREQ(N)*DT)
      S1=SIN(FREQ(N)*DT)
      CC=1.0
      SC=0.0
      DO 36 M=2,MLAGM1
      CT=CC*C1-SC*S1
```

```
      ST=SC*C1+CC*S1
      CC=CT
      SC=ST
      SUM1=SUM1+SPHI(M)*CC
   36 SUM2=SUM2+APHI(M)*SC
      CSPEC(N)=SUM1/XMLAG
   40 QSPEC(N)=SUM2/XMLAG
  101 FORMAT(4X,10H FREQUENCY,4X,15H AUTO-SPECTRUM1,3X,15H AUTO-SPECTRUM
     12,3X,12H CO-SPECTRUM,2X,14H QUAD-SPECTRUM,3X15H  WAVE PERIOD  ,
     2'   PHASE    ','  COHERENCE',//)
  102 FORMAT(4X,F8.5,7X,E13.7,6X,E12.7,5X,E13.7,6X,E12.5,3X,F10.5,3X,
     1F10.5,3X,F10.5)
  103 FORMAT    (9X,49H SMOOTHED(PARZEN  WINDOW) ENERGY SPECTRAL DENSITY
     1///)
  104 FORMAT(3X,10H (CYC/SEC), 6X,7H  M2/HZ)
      WRITE(6,803) DATE,HOUR
      WRITE(6,110)
      WRITE(6,111)(TAU(M),PHN2(M),M=1,MLAG)
      WRITE(6,103)
      WRITE(6,101)
      WRITE(6,104)
      DO 17 I = 1,NFREQ
      PHASE(I) = ATAN( QSPEC(I)/ CSPEC(I))*180.0/3.146
      IF( CSPEC(I).LT.0.0)PHASE(I)=PHASE(I) + 180.0
      IF(PHASE(I).GT.180.0) PHASE(I) = PHASE(I) - 360.0
      COHER(I)=((QSPEC(I)*QSPEC(I)+CSPEC(I)*CSPEC(I))/(SQRT(SPEC(I)*SPEC
     1(I)*SPE2(I)*SPE2(I))))
   17 CONTINUE
      WRITE(6,102)(CYCL(M),SPEC(M),SPE2(M),CSPEC(M),QSPEC(M),PER(M),
     1PHASE(M),COHER(M),M=1,NFREQ)
      WRITE(6,113)
      WRITE(6,114)(CYCL(M),SPE2(M),WSPEC(M),PER(M),RESPF(M),XK(M),M=1,NF
     1REQ)
C     CALL DRAW TO PLOT PHASE ANGLE AS A FUNCTION OF FREQUENCY
      CALL DRAW(175,CYCL,PHASE,0,0,LABEL5,ITITIL,0.1,180.0,1,0,2,0,6,2,0
     1,LAST)
C     CALL DRAW TO PLOT COHERENCE
      CALL DRAW(175,CYCL,COHER,0,0,LABEL6,ITITLI,0.1,1.0,0,0,0,0,6,1,0,L
     1AST)
      DO 6969 IL=1,NFREQ
       SPEC(IL)=ALOG10(SPEC(IL))
       SPE2(IL)=ALOG10(SPE2(IL))
 6969 CONTINUE
      CALL DRAW(175,CYCL,SPE2,1,0,LABEL7,ITITLL,0.1,1.0,9,0,2,0,6,9,0,LA
     1ST)
      CALL DRAW(175,CYCL, SPEC,3,0,LABEL8,ITITLL,0.1,1.0,9,0,2,0,6,9,0,L
     1AST)
      GO TO 530
```

```
  743 CONTINUE
      WRITE(6,107)(TAU(M),PHN(M),M=1,MLAG)
C     CALL DRAW TO PLOT SPECTRUM
      CALL DRAW(480,TAU,  PHN,0,0,LABEL,ITITEL,0.0,0.2,2,0,2,0,8,8,1,
     1LAST)
  105 FORMAT (10X,24H ENERGY SPECTRAL DENSITY///,5X,10H FREQUENCY,5X,13H
     1      SPECTRUM)
  106 FORMAT (5X,F10.5,6X,E12.6)
  107 FORMAT(5X,F10.6,6X,F10.6,6X,F10.6)
      WRITE(6,105)
      WRITE(6,106)(CYCL(M),SPEC(M)        ,M=1,NFREQ)
  108 FORMAT(2F10.8)
  109 FORMAT (I6)
  110 FORMAT('LAG TIME CROSS CORRELATION FN',//)
  111 FORMAT(5X,F10.6,6X,F10.6)
  112 FORMAT('0',7X,'LAGTIME',8X,'AUTO 1',11X,'AUTO 2',//)
  113 FORMAT('0',4X,10H FREQUENCY,9X,6H W ACT,11X,7H W THEO, 9X,11HWAVE
     1PERIOD,6X,5HRESPF,18X,1HK,//)
  114 FORMAT(4X,F8.5,7X,E12.7,7X,E12.7,7X,F10.5,6X,E12.6,6X,E12.6)
  888 RETURN
  999 STOP
      END
C SUBROUTINE TO CONVERT PRESSURE SPECTRUM TO ENERGY SPECTRUM

      SUBROUTINE PRESS(FREQ,SPEC,WSPEC,NFREQ,RESPF,XK,H,X2,DF,FB,FMAX)
      DIMENSION FREQ(NFREQ),SPEC(NFREQ),WSPEC(NFREQ),RESPF(NFREQ)
      DIMENSION XK(NFREQ)
      NMAX = (FMAX-FB)/DF+1.0
      DO 11 I=1,NMAX
C CALCULATE LINEAR WAVE LENGTH BY NEWTONS METHOD
      IF(FREQ(I)-0.00001) 8,8,7
    7 XKHO = FREQ(I)*FREQ(I)*H/9.80
      IF(XKHO-6.3) 5,1,1
    1 XKH = XKHO
      GO TO 9
    5 XKH = SQRT(XKHO)
    3 SH = SINH(XKH)
      CH = COSH(XKH)
      EPS = XKHO-XKH*SH/CH
      SLOPE = -XKH/CH**2-SH/CH
      DXKH = -EPS/SLOPE
      IF(ABS(DXKH/XKH)-0.0001) 9,9,4
    4 XKH = XKH +DXKH
      GO TO 3
    8 RESPF(I) = 1.00
      GO TO 11
    9 XK(I) = XKH/H
```

```
      IF(XK(I).LE.2.0) GO TO 14
      RESPF(I) = 1.0
      GO TO 11
   14 RESPF(I)  = FREQ(I)*(SINH(XK(I)*(H-X2))/SINH(XK(I)*H))
   11 WSPEC(I)  = RESPF(I)*RESPF(I)*SPEC(I)
      WRITE(6,117)
  117 FORMAT('0',6X,5HSIGMA,12X,4HSPEC,14X,6HW THEO,13X,7HRESPFCT,8X,
     18HWAVE NO.,//)
      WRITE(6,118)(FREQ(I),SPEC(I),WSPEC(I),RESPF(I),XK(I),I=1,NMAX)
  118 FORMAT(4X,F8.5,7X,E12.7,7X,E12.7,7X,E12.7,7X,E12.7)
   12 RETURN
      END


      SUBROUTINE TREND(FX,NTS,DT,CALXX)
      CIMENSION FX(NTS)
C CALIBRATICNG RECORD
      CO 104 I=1,NTS
  104 FX(I) = FX(I)*CALXX
C CCMPUTING THE LINEAR TREND
      FNTS = NTS
      SUMF = 0.0
      DO 101 I=1,NTS
  101 SUMF = SUMF + FX(I)
      SUMF1 = 0.0
      DO 102 I=1,NTS
      XI = I
  102 SUMF1 = SUMF1 + XI*FX(I)
      XNM1 = NTS-1
      XNP1 = NTS+1
      XM = (1.0/DT)*(12.0*SUMF1/(FNTS*XNM1*XNP1)-6.0*SUMF/(XNM1*FNTS))
      B = SUMF/FNTS-XM*XNP1*DT/2.0
      FMEAN = SUMF/FNTS
      WRITE(6,9) FMEAN,XM,B
    9 FORMAT (3X,8H MEAN = ,F10.5,3X,9H SLOPE = ,F10.5,3X,13H INTERCEPT
     1= ,F10.5//)
      DO 103 I=1,NTS
      XI = I
  103 FX(I) = FX(I) - (B+XM*XI*DT)
      RETURN
      END


      SUBROUTINE SMO(MD,X1,X2,NFREQ)
      DIMENSION X1(MD),X2(MD)
      DO 1 N=1,MD
      NA=N+MD
      NN=NFREQ-N+1
```

```
      NB=NN-MD
      X2(N) = 0.25*(X1(1)+X1(NA))+0.5*X1(N)
    1 X2(NN)=0.5*(X1(NN)+X1(NB))
    3 MB=MD+1
      ME=NN-1
    5 DO 2 N=MB,ME
      NA=N+MD
      NB=N-MD
    2 X2(N)=0.25*(X1(NA)+X1(NB))+0.5*X1(N)
      RETURN
      END


      SUBROUTINE AVER (FX,NTS,DT)
C SUBROUTINE FOR CALCULATING TURBULENT INTENSITY, URMS
      DIMENSION FX(NTS)
      U2 = 0.0
      SUMU2 = 0.0
      DO 151 I=1,NTS
      U2 = FX(I)*FX(I)
      SUMU2 = SUMU2 + U2
  151 CONTINUE
      FNTS = NTS
      U2 = SUMU2/FNTS
      URMS = SQRT(U2)
      WRITE(6,152) U2,URMS
  152 FORMAT (3X,6H H2 = ,F10.5,3X,8H HRMS = ,F10.5,5H  M   )
CCMPUTING AVERAGE PERIOD, T
CCUNTS THE TOTAL ZERO UP-CROSSINGS
      USUM = 0.0
      K = 1
   68 N = K
   69 N = N+1
      IF(FX(N)) 73,69,69
   73 K=N
   71 K = K+1
      IF(FX(K))71,71,80
   80 USUM = USUM + 1.0
      IF(NTS-K) 83,83,68
   83 T = FNTS*DT/USUM
      WRITE(6,82) T
   82 FORMAT (3X,18H AVERAGE PERIOD = ,F10.5,4H SEC//)
      RETURN
      END
```

```
      SUBROUTINE HAMM(MLAG,PHI)
C   HAMM SUBROUTINE HAMMING LAG WINDOWS THE AUTO-CORRELATION FUNCTION
      DIMENSION PHI(MLAG)
      PI = 3.14159265
      XMLAG = MLAG
      DO 31 M=1,MLAG
      R = M
      UM = 0.54 + 0.46*COS(PI*R/XMLAG)
      PHI(M ) = PHI(M )*UM
   31 CONTINUE
      RETURN
      END

      SUBROUTINE PARZ(MLAG,PHI)
C     PARZ SUBROUTINE PARZEN FILTERS AUTO-CORRELLATION FUNCTION
      DIMENSION PHI(MLAG)
      XMLAG = MLAG
      MLAGH = XMLAG/2.0-0.1
      MLAGH1 = MLAGH + 1
      DO 31 M=1,MLAGH
      MM = M-1
      R = MM
      RM = R/XMLAG
      UM = 1.0-6.0*RM*RM*(1.0-RM)
      PHI(M ) = PHI(M )*UM
   31 CONTINUE
      DO 32 M = MLAGH1,MLAG
      MM = M-1
      R = MM
      RM = R/XMLAG
      RM1 = (1.0-RM)
      UM = 2.0*RM1*RM1*RM1
      PHI(M ) = PHI(M )*UM
   32 CONTINUE
      RETURN
      END
```

BIBLIOGRAPHY

1. Seymour, H. A., Statistical Relations Between Salinity, Temperature and Speed of Sound in the Upper Ocean, M.S. Thesis, Naval Postgraduate School, Monterey, California, 1972.

2. Duchock, C. J., Jr., The Measurement and Correlation of Sound Velocity and Temperature Fluctuations Near the Sea Surface, M.S. Thesis, Naval Postgraduate School, Monterey, California, 1972.

3. Bordy, W. B., Spectral Measurements of Water Particle Velocities Under Waves, M.S. Thesis, Naval Postgraduate School, Monterey, California, 1972.

4. Haley, M. C., Small Scale Interactions in the Near Surface Ocean, M.S. Thesis, Naval Postgraduate School, Monterey, California, 1972

5. Whittemore, M.A.N., Small Scale Temperature Fluctuations Near the Sea Surface, M.S. Thesis, Naval Postgraduate School, Monterey, California, 1973.

6. Gossner, J., Comparison of Measured and Calculated Sound Velocity Near the Sea Surface, M.S. Thesis, Naval Postgraduate School, Monterey, California, 1973.

7. Krapohl, R. F., Wave Induced Water Particle Motion Measurements, M.S. Thesis, Naval Postgraduate School, Monterey, California, 1972.

8. Barakos, P. A., The Effects of Internal Tides in Shallow Water Acoustics, Paper for 84th Meeting of Acoustical Society of America, Naval Undersea Center, San Diego, California, 1972.

9. Fitzgerald, J. R., Statistical Study of Sound Speed in the Inhomogeneous Upper Ocean, M.S. Thesis, Naval Postgraduate School, Monterey, California, 1972.

10. Alexander, C. H., Sound Phase and Amplitude Fluctuations in an Anisotropic Ocean, M.S. Thesis, Naval Postgraduate School, Monterey, California, 1972.

11. McKendrick, J. D. III, An Investigation of Digital Spectral Analysis Programs and Computer Methods Utilized at NPS in Analysis of High Frequency Random Signals, M.S. Thesis, Naval Postgraduate School, Monterey, California, 1972.

INITIAL DISTRIBUTION LIST

		No. Copies
1.	Defense Documentation Center Cameron Station Alexandria, Virginia 22314	2
2.	Library, Code 0212 Naval Postgraduate School Monterey, California 93940	2
3.	Oceanographer of the Navy The Madison Building 732 N. Washington Street Alexandria, Virginia 22217	1
4.	Department of Oceanography Naval Postgraduate School Monterey, California 93940	3
5.	Commander, Navy Ship Systems Command Code 901 Department of the Navy Washington, D. C. 20305	1
6.	Dr. Ned A. Ostenso Code 480 D Ocean Science and Technology Division Office of Naval Research Arlington, Virginia 22217	1
7.	Program Director / Physical Oceanography Code 481 Ocean Science and Technology Division Office of Naval Research Arlington, Virginia 22217	1
8.	LCDR Jon W. Carlmark (USN) Project Office Code 485 Ocean Science and Technology Division Office of Naval Research Arlington, Virginia 22217	1
9.	Professor H. Medwin, Code 61 Department of Physics Naval Postgraduate School Monterey, California 93940	1

		No. Copies
10.	Dr. Noel E. Boston, Code 58 (thesis advisor) Department of Oceanography Naval Postgraduate School Monterey, California 93940	3
11.	Dr. E. B. Thornton, Code 58 Department of Oceanography Naval Postgraduate School Monterey, California 93940	1
12.	Lt. W. J. Frigge, USN (Student) USS Aylwin (DE-1081) FPO, New York, N.Y. 09501	1

Security Classification

DOCUMENT CONTROL DATA - R & D

(Security classification of title, body of abstract and indexing annotation must be entered when the overall report is classified)

1. ORIGINATING ACTIVITY (Corporate author) Naval Postgraduate School Monterey, California 93940	2a. REPORT SECURITY CLASSIFICATION Unclassified 2b. GROUP

3. REPORT TITLE

Shallow Water Experiment Utilizing the STD MODEL 9006 at a Fixed Point

4. DESCRIPTIVE NOTES (Type of report and, inclusive dates)

5. AUTHOR(S) (First name, middle initial, last name)

William Joseph Frigge

6. REPORT DATE	7a. TOTAL NO. OF PAGES	7b. NO. OF REFS
March 1973	83	11

8a. CONTRACT OR GRANT NO.	9a. ORIGINATOR'S REPORT NUMBER(S)
b. PROJECT NO.	
c.	9b. OTHER REPORT NO(S) (Any other numbers that may be assigned this report)
d.	

10. DISTRIBUTION STATEMENT

Approved for public release; distribution unlimited.

11. SUPPLEMENTARY NOTES	12. SPONSORING MILITARY ACTIVITY
	Naval Postgraduate School Monterey, California 93940

13. ABSTRACT

An examination of the salinity sensing capabilities of the STD Model 9006 was made in laboratory and in shallow water field conditions both in Monterey Bay and at the N.U.C. Tower off Mission Beach at San Diego, California. Laboratory studies showed it to be influenced by changes in water velocity from zero to non-zero. Field studies showed that the instrument was unsuitable for sensing instantaneous microstructure fluctuations of salinity in shallow water while being held at a single depth in a wave influenced regime. Averaged over a period of ten seconds or more, however, the output of the instrument was judged to be accurate to at least the first decimal place.

DD FORM 1473 1 NOV 65 (PAGE 1)

S/N 0101-807-6811

Security Classification

A-31408

Security Classification

14 KEY WORDS	LINK A		LINK B		LINK C	
	ROLE	WT	ROLE	WT	ROLE	WT
STD Model 9006						
Salinity						
Temperature						
Sound velocity						
Energy density spectra						
Coherence spectra						
Phase spectra						

DD FORM 1 NOV 65 1473 (BACK)

S/N 0101-807-6821

Security Classification

A-31409

Thesis
F8925 Frigge 145928
c.1
Shallow water experiment utilizing the STD Model 9006 at a fixed point.